Technical University of Crete
School of Electrical and Computer Engineering

Diploma Thesis

Optimal Operation of Energy Systems of Groups of Large Buildings

Farinis Georgios

EXAMINING COMMITTEE

Associate Professor Kanellos Fotios (Supervisor)

Professor Kalaitzakis Konstantinos

Associate Professor Koutroulis Eftychios

Chania February 2020

Acknowledgment

I would like to express my gratitude and thank my supervisor, Assoc. Prof. Kanellos Fotios, for the opportunity that he gave me to work on this project and for his guidance and support during all this time preparing my master thesis. I am also grateful to Prof. Kalaitzakis Konstantinos and Assoc. Prof. Koutroulis Eftychios for serving on my thesis committee. Finally, I would like to thank my family and my friends that are close to me for their love, support and patience.

Abstract

The development of microgrids has enabled prosumers to develop optimal power management and demand response (DR) strategies. Based on this idea, virtual prosumers and microgrids can be created in a traditional city structure, exploiting microgrids' ability to operate connected or disconnected to the grid. Therefore, the development of more complex energy control and management systems becomes necessary.

In this thesis, an easy to apply and computationally efficient energy management system (EMS) has been developed in Matlab. It is based on a hierarchical multi-agent system aiming to minimize the operating cost of a microgrid, that consists of a group of buildings, renewable energy sources (RES), energy storage systems (ESS) and electric vehicles (EVs). The examined optimization problem is solved using the particle swarm optimization algorithm (PSO), that ensures the optimum use of every microgrid's component. Based on the results obtained by applying the algorithm to the operation of the microgrid, both in the time frame of one day and one week, cost savings of 40% can be achieved while all the microgrid's energy needs and operation constraints are met.

Contents

1. INTRODUCTION

1.1 General

In recent years, the increase in the global population and the concentration of large numbers of people in urban areas made necessary the development of large-scale buildings used for several types of activities. Buildings of this type are large consumers of electricity while they usually comprise integrated electric power generation and energy storage units.

There are many different ways to reduce energy use, from simple behavioral adjustments to extensive home improvements. Replacing light bulbs and using smart power strips are some simple changes to reduce energy consumption, while upgrading the heating ventilation and air conditioning (HVAC) system and installing a programmable or smart thermostat is an expensive one. Energy management systems (EMSs) is a method of saving energy that combines monitoring, controlling and optimizing the use of electricity during the day. Implementation of this requires the integration of sensors, microcontrollers and software into the existing system so that human activity and external weather can be monitored in order to make the optimum decision on the use of electricity in order to reduce it and lead to cost reduction.

Many countries have introduced EMSs into their market with USA having more than US$2b in revenue. China and Germany are following with US$1,3b and US$681m respectively while UK and South Korea are fulfilling the top five list with US$457m and US$326m each. Currently the average revenue per smart home in the energy management segment amount to US$77. Worldwide revenue is expected to show an annual growth rate of 14.4%, resulting in a market volume of US$12,442m by 2024.

1.2 This Thesis Subject

Energy management systems (EMSs) usually focus on managing and controlling a single building microgrid to optimize its operation [1,2,6,7]. In other cases, they focus more on controlling a type of load that can be either the thermal load of a building or the electrical load [8-9]. While, some don’t include electric vehicles [10-11]. The characteristic of these algorithms is their large execution time, limiting them to making only one optimized forecast per day.

The energy management method proposed in this thesis deals with all the of optimization processes of building prosumer microgrid. All of these buildings include renewable energy sources (RESs) as well as energy storage units (ESUs), which the system is also called upon to utilize appropriately to guarantee cost-optimal operation. Its introduction is easy and mainly pose no risk as it takes advantage of the already existing structure of a building network. As it was designed, large building prosumers can have over 40% cost savings.

In order to achieve this magnitude of energy saving, the system relies on various types of forecasts relating to human activity but also to changing environmental conditions. It also considers the change in electricity price during the day. So, knowing the electricity price changes and needs of the grid, decisions are made regarding the purchase and sale of energy from and to the grid.

The goal of the proposed algorithm is to minimize the operating costs of prosumers, meeting their energy needs. Its advantage is that due to its short execution time it can be used as a forecasting algorithm but also in real time application.

1.3 Thesis Overview

In Chapter 2, the definition of energy management systems and building automation systems is given. While, Chapter 3 focused on the microgrid definition, the components that a microgrid consists of, the devices and the algorithms that can be used to control a microgrid. In Chapter 4 is given an introduction of the proposed energy management system, the description of the microgrid models, the optimization objective functions and the proposed algorithm overview. Simulation results are provided in Chapter 5 for a set of different scenarios and finally in Chapter 6 are given the conclusions derived from the results.

2. ENERGY MANAGEMENT

Automatic building control has developed through the years, leading into automated energy control systems that are used today in a variation of applications. Every nonresidential building in today's world have automatic controllers, that use processors, to control lighting, hot water or air-conditioning devices. The combination of different types of control systems can be called energy management systems (EMSs), energy management control systems (EMCSs) or building automation systems (BASs). Companies have adopted these technologies in order to abate the buildings' operating costs and improve heating, ventilation, air-conditioning (HVAC), lighting system use and for reducing energy use.

2.1 Energy Management Systems

An EMS is a system of computer-aided tools used by operators of electric utility grids to monitor, control, and optimize the performance of the generation and transmission system. It is also used in small scale systems like microgrids for the generation and consumption of the energy. Recently cloud-based EMSs are used for remote control of an HVAC or energy consuming devices, collect real time data from these devices and optimize real-time their use in order to save energy.

2.2 Building Automation Systems

BAS core functionality keeps building climate within a specified range, provides light to rooms based on an occupancy schedule (in the absence of overt switches to the contrary), monitors performance and device failures in all systems, and provides malfunction alarms to building maintenance staff. A BAS should reduce building energy and maintenance costs compared to a non-controlled building. Most commercial, institutional, and industrial buildings built after 2000 include a BAS. Many older buildings have been retrofitted with a new BAS, typically financed through energy and insurance savings, and other savings associated with pre-emptive maintenance and fault detection.

Almost all green buildings are design to accommodate a BAS for the energy, air and water conservation characteristics. Electrical device demand response is a typical function of a BAS, as is the more sophisticated ventilation and humidity monitoring required of "tight" insulated buildings. Most green buildings also use as many low-power DC devices as possible. Even a passive house design intended to consume no net energy what so ever will typically require a BAS to manage heat capture, shading and venting, and scheduling device use.

3.
MICROGRID

3.1 Microgrid Definition

A microgrid is a group of loads and energy resources that acts as a single controllable entity with respect to the grid. A microgrid can operate connected to the synchronous grid, but also can be disconnected to "island-mode" operating autonomously.

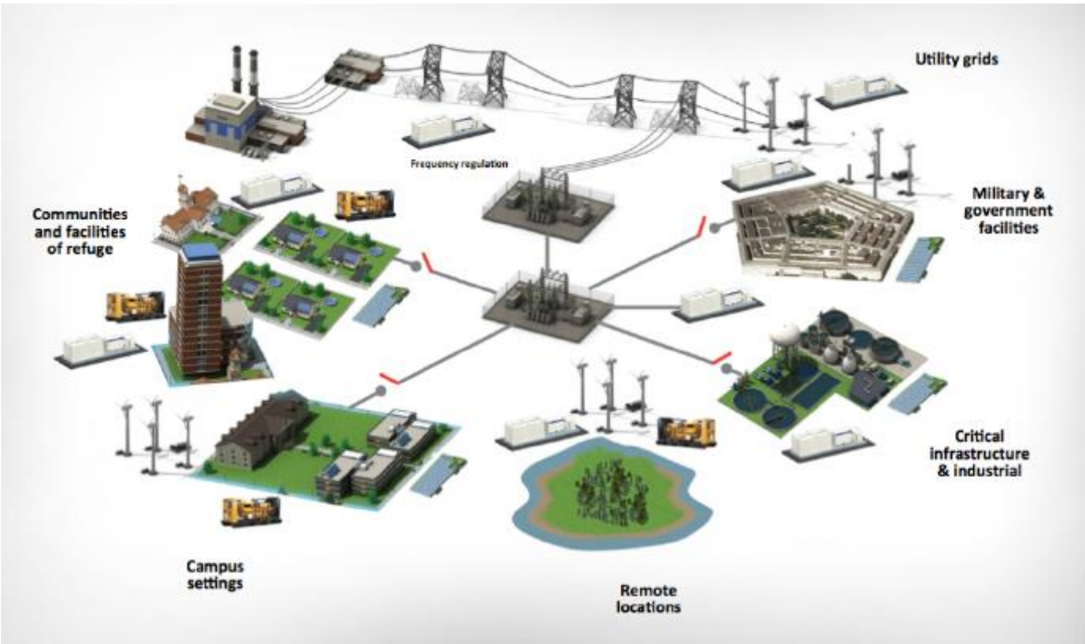

Figure 3.1

Microgrids are electricity distribution systems containing loads and distributed energy resources, that can be operated in a controlled, coordinated way either while connected to the main power network or while is landed. This way, microgrids are able to switch stated and supply emergency power to the grid, or receive power from it.

A microgrid consists of many elements that vary in each case, based on its location and usage. These elements are divided into the following categories:

- **Generators** covers all sources possible within the context of a microgrid, like fossil or biomass-fired small-scale combined heat and power (CHP), photovoltaic modules (PVs), small wind generator (WG), mini-hydro, etc.
- **Storage devices** includes all of electrical, pressure, gravitational, flywheel, and heat storage technologies.
- **Loads** cover a wide range of electrical and thermal loads. Electrical loads derive from plug-in devices of controllable electrical appliances, while thermal loads refer to the cooling or heating system.

There are several types of microgrids, as shown in Figure 3.1, for different applications that continue to evolve during the market and technology changes. Some types of microgrids are the following:

- **Campus Microgrids** could refer to corporate campuses or university campuses. This kind of microgrids are located in tight geography, consist of a number of generator and loads, making them easy to manage.
- **Community Microgrids** can serve up to a few thousands of households, meeting all their energy needs. Consumers in this microgrids can have their own renewable energy sources, whose power production can distribute throughout the community. The community microgrid may also have a centralized or several distributed energy storage (DS) unites making them able to be in the form of an AC and DC system. In the developing world, community microgrids can be used to achieve electrification for the first time. In the developed world they are often used to help communities achieve renewable energy targets.
- **Island Microgrids** are built in areas that are far distant from any transmission and distribution infrastructure and have no connection to the utility grid. The high cost of importing liquid fuels, defined these microgrids as a viable solution. While traditionally, macrogrid run off diesel, small and large islands around the world are incorporating renewables and energy storage into their energy systems.
- **Remote Microgrids** are similar to island microgrids, but describe a broader category. As, these microgrids are designed to be self-sufficient, due to changes in production from renewables, shortfall or excessive power generation can be caused. This will result into unacceptable voltage or frequency deviation in the microgrids. Therefore, these neighboring networks can be interconnected in order to exchange power and improve the voltage and frequency deviations. Like island microgrids, remote microgrids were traditionally dominated by diesel but are rapidly incorporating solar plus storage.
- **Commercial and Industrial Microgrids** are in use because of the power supply reliability and security they offer. In most of the industries, a manufacturing process interruption can cause a huge cost increase and start up time delays to the production. Thus, a microgrid can be designed with RESs and ESUs that are being controlled locally and prevent this kind of interruptions.
- **Military Microgrids** are being actively deployed with focus on both physical and cyber security for military facilities in order to assure reliable power without relying on the utility grid. Due to being so expensive and dangerous to transport liquid fuels to remote areas and through hostile regions, military microgrids have integrated system of energy production

and energy storage making them able to operate for large period of times without fossil fuels.

The above types of microgrids are used to ensure their proper functioning so as to better serve the energy needs of customers by ensuring the most economical operation possible, ensuring an ecological solution to power supply. Some of microgrids' advantages are:

- The capability of operating in island mode and grid-connected mode and the ability to switch between these two modes. In grid-connected mode, the microgrid can trade power with the utility grid. Therefore, these loads can balance microgrid energy need of cover utility grid's demand of energy. In island mode, RES generate power that covers the load demand of customers or is provided to the ESUs for future use.
- The reduction of carbon emissions while RESs are able to generate power and by using the traditional methods of power generation otherwise.
- The security of being damaged from natural disasters by not having miles of above-ground wires and other electric infrastructure that needs to be maintained or repaired following these events.

Nonetheless, there are some challenges related to the operation of microgrids. Some of them are:

- The bidirectional power flows that are caused by distributed generation (DG) units in the network at low voltage levels that may lead to complications in protection coordination, undesirable power flow patterns, fault current distribution and voltage control.
- The stability issues exiting because of the interactions between control system of DG units. These interactions may create local oscillations, requiring a thorough small-disturbance stability analysis. Moreover, the switchover process between grid-connected mode and island mode of the microgrid can create transient instability.
- The low inertia in the system can lead to severe frequency deviations in island mode operation if a proper control system is not implemented. The low inertia characteristic is more evident when power electronic DG units exist in the microgrid.
- The uncertainty for the operation of microgrids. These uncertainties are related to the load profiles of customers and the weather forecast, that can cause failure in supply-demand balance. Traditional grids do not face this kind of problems, due to the large amount of energy they possess.

3.2 Microgrid Components

A set of components can define a microgrid. These components vary depending on the type of microgrid and the activity of the scorpions. Thus, a microgrid can be analyzed in the buildings that it consists of, other loads that burden the local grid, in the RES that it contains, in its ESUs and finally in the network to which it is connected and interacts with.

3.2.1 Buildings

In a microgrid there are various types of buildings that serve a set of consumer needs. These buildings can be divided into some broader categories according to their usage as follows:

- **Residential Buildings** facilitate activities such as sleeping, living and cooking. The building must include one or more family residencies, apartments, flats and private garages.

- **Educational Buildings**, housing educational institutions such as schools or colleges which are affiliated and recognized by an appropriate board, university or any similar affiliation authority.
- **Institutional Buildings** consist of buildings that are constructed by the government, semi-government organizations or registered trusts for specific purposes. Those specific purposes include medical treatment purposes such as treatment of physical or mental illness, children's hospitals, old age homes, centers for the care of orphans or abandoned women, etc.
- **Assembly Buildings** are defined as buildings or parts of them which houses public gatherings congregated with the intent of amusement, recreation, social, religious, patriotic, civil, travel or other similar purposes.
- **Business Buildings** are used for keeping records of business transactions, maintaining accounts, bookkeeping purposes or managing other types of records then it can be classified as a business building.
- **Mercantile Buildings** are used for housing shops, stores or showrooms where display and sale of wholesale goods, retail goods or merchandise is carried out.
- **Industrial Buildings** used to manufacture, assemble or process products or materials.
- **Storage Buildings** are used for the storage of commodities, goods, merchandise, etc.
- **Wholesale Establishments** include establishments being fully or partially utilized for wholesale trade and manufacture, wholesale shops having required storage facilities or warehouses and establishments providing truck transportation services or truck transportation booking services.
- **Mixed Land Use Buildings** are buildings which are used for both residential purposes as well as for carrying out non-residential activities.
- **Hazardous Buildings** have been further divided into two sub-categories as:
    - Buildings used for the manufacture, processing, handling or storage of substances which are radioactive, highly combustible/explosive or capable of burning rapidly with/without the potential to produce poisonous fumes or emissions that are explosive in nature.
    - Buildings used for the manufacture, processing, handling or storage of substances which are highly corrosive, toxic or noxious alkalis, acids or other chemicals producing explosive or poisonous fumes, explosive mixtures or substances capable of disintegrating matter into fine particles causing spontaneous ignition.

Buildings can also be divided into some basic categories based on their energy savings as:

- **Low energy buildings** term is used to describe a building that uses less energy than a conventional structure, but not quite enough to be considered a net zero-energy buildings (NZEBs).
- **Passive buildings** consume hardly any energy for heating, cooling and appliances. They are similar to NZEB, but they don't utilize integrated RES supply systems and other energy generation technologies.
- **Net zero energy buildings** (NZEBs) produce the amount of energy that they have in demand for the rime period of a year. NZEBs are defined by a building design that minimizes the energy demand and renewable energy systems that meet their energy needs.

- **Plus energy buildings** consistently produce more energy than they consume. They inject the generated energy back into the main grid at a price set by energy providers, or this energy is stored in their energy storage system for future exploitation.

3.2.2 Photovoltaic system

The development of technology has also led to the improvement of photovoltaic devices, making them better in performance but also lowering their manufacturing costs. This proves the fact that whilst the price of PVs for residential use in 2014 was US$3,49 per watt, in 2018 the residential use price dropped to US$2,7 per watt. Efficiency-wise, in 2014 the average solar panel was by 15% efficient and in 2018 this number came up to almost 20%.

Some of the advantages of using PVs are:

- The environmentally friendly solution PVs offer by not aggravating the air and water pollution problem.
- The noise free operation of these units.
- The long lifetime they have and the reduced maintenance needs.

However, the technology of PV systems present some drawbacks.

- Manufacturing and installation costs are high, compared to other energy sources.
- PVs have low efficiency rates.
- PVs' efficiency rated depend on the weather, dirt and shading conditions.
- The manufacturing process of PVs use some toxic chemical.

3.2.3 Wind generators

A WG converts the kinetic energy in wind into mechanical energy that moves a rotating shaft and threw the generator is converted into electrical energy. Wind turbines have become an important and reliable renewable energy source in many countries that aim to become energy-independent and reduce the use of liquid fuels. According to Betz Limit's law, the maximum theoretical limit of energy efficiency is 59.3%. Currently, wind energy efficiency is varying between 35% and 45%.

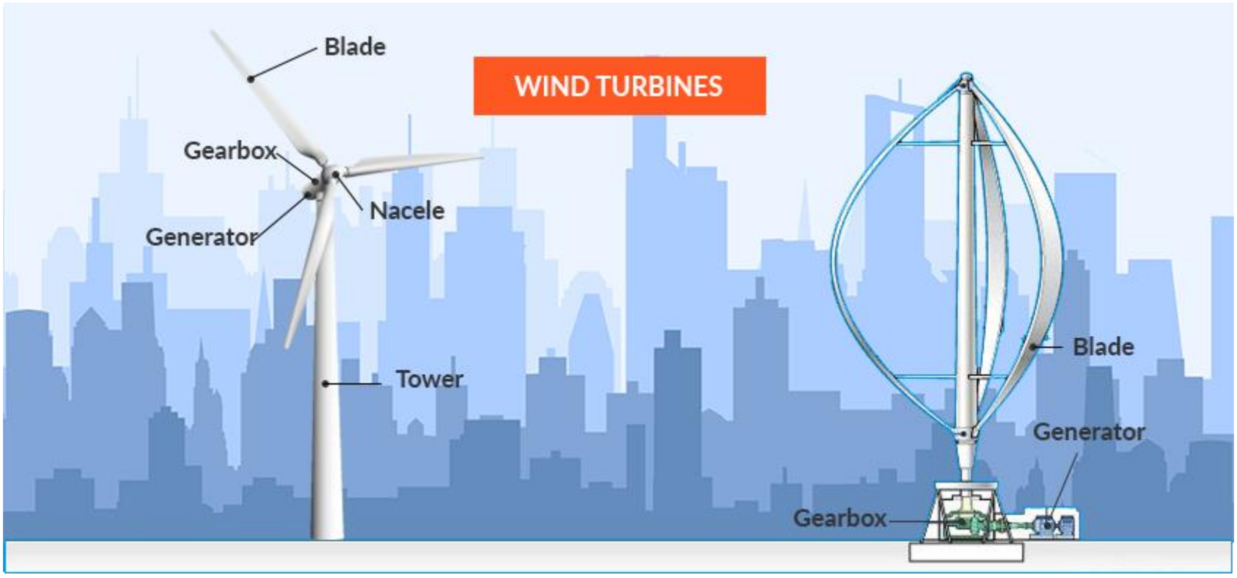

Figure 3.2 HAWT and VAWT (Darrieus) type of wind generators. Source: Let's Go Solar.

There are several types of WGs developed in recent years as companies seek to draw greater efficiency from their designs. Some of these designs include:

- **Horizontal axis**
  Large three-bladed horizontal-axis wind turbines (HAWT) with the blades upwind of the tower produce the overwhelming majority of wind power in the world today. These turbines have the main rotor shaft and electrical generator at the top of a tower, and must be pointed into the wind. Turbines used in wind farms for commercial production of electric power are usually three-bladed. These have low torque ripple, which contributes to good reliability.
- **Vertical axis** wind turbines (VAWTs) have the main rotor shaft arranged vertically. The main advantage of this arrangement is that the turbine does not need to be pointed into the wind to be effective. Therefore, this type of WT can be used in places that the wind speed varies and onto buildings that the wind direction varies.
- **Darrieus** turbines, were named after the French inventor, Georges Darrieus. They have good efficiency, but produce large torque ripple and cyclical stress on the tower, which contributes to poor reliability. They also generally require some external power source, or an additional Savonius rotor to start turning, because the starting torque is very low. The torque ripple is reduced by using three or more blades, which results in greater solidity of the rotor.
- **H-Rotor**
  A subtype of Darrieus turbine with straight, or curved, blades. The cyclo-turbine variety has variable pitch to reduce the torque pulsation and is self-starting.

Figure 3.3 H-Rotor wind turbine. Source: Klein-Windkraftanlagen.

- **Savonius** wind turbines are drag-type devices with two, or more, scoops. They are always self-starting if there are at least three scoops. Twisted Savonius is a modified savonius, with long helical scoops to provide smooth torque. This is often used as a rooftop wind turbine and has even been adapted for ships.

Figure 3.4 Savonius wind turbine. Source: Researchgate (G. Ragul).

- **Parallel**
  The parallel turbine is similar to the crossflow fan or centrifugal fan. It uses the ground effect.

The challenges of using WGs mostly refer to:

- The high buying and installing cost of them.
- The noise caused by them and aesthetics.
- The non-profitable use of the land, compared to other uses.

Despite the disadvantages, wind energy is one of the largest sources of energy in Europe, covering a total of 14% of energy needs in 2018. Denmark has the highest wind energy demand coverage with 41%, followed by Ireland with 28% and Portugal with 24%. Germany, Spain and the UK follow with 21%, 19% and 18% respectively.

3.2.4 Energy storage

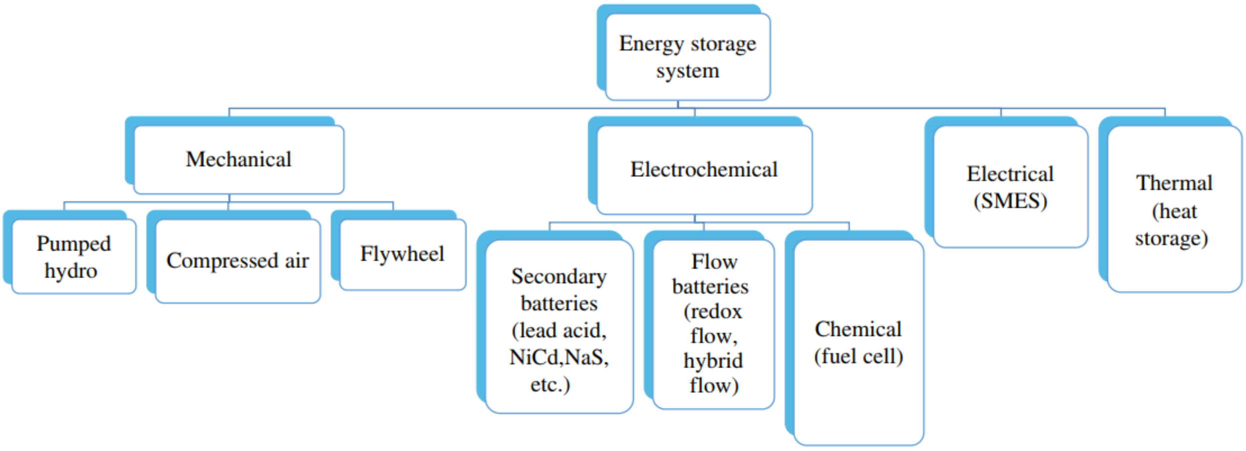

Figure 3.5 Type of energy storage systems. Source: Fraunhofer ISE.

Energy storage systems (ESSs) play a very important role in microgrids, improving their operation. Due to the instability of energy production through RESs, it is difficult to keep the microgrid operating smoothly, especially in islanded mode. As an ESS can operate as a load or generator when it is in charging or discharging mode, it is able to balance the power in the microgrid and reduce the impact of any fluctuation. This improves the stability of the microgrid significantly.

There are several types of ESSs that can be used in a microgrid.

- **Batteries**
  Lead-Acid, Lithium-Ion, Redox-Flow and Sodium are the main types that are commonly used in the industry. With Lead-Acid being suitable for uninterrupted power supply as its low cost and high efficiency. Lithium-ion batteries usually are used in small electronic devices, due to their small self-discharge rate, having great potential for electric vehicle use. Redox-Flow batteries present a long lifetime of 40 years and easy electrolyte exchange, making them capable of use into electric vehicles. Sodium batteries' advantage is their high-power density, long battery lifetime and high efficiency.
- **Flywheel** is a disk with a certain amount of mass that can store energy into kinetic form by spinning. This way, flywheels have high power density, high conventional efficiency and long life-span.
- A **supercapacitor** used in a microgrid as and ESU needs a stack of single cells connected in series. Supercapacitors present high power density and high energy convention efficiency.
- **Pumped hydroelectric energy storage** is another energy storage method using gravitational energy of water that is pumped from a lower elevation level to a higher one when energy need to be stored and vice versa when energy needs to be extracted. Pumped storage is the largest capacity form of grid energy storage available.
- **Fuel cells** are devices which take stored chemical energy and converts it to electrical energy directly. Their use is best when combined with hydrogen as fuel, however hydrogen is hard to produce. Fuel cells present a high energy convention efficiency and are suitable for long duration energy storage.

When designing a microgrid ESS, it is necessary to consider all the advantages and disadvantages of the technologies mentioned in order to achieve the best balance of energy density, power density, response time and lifetime.

3.2.5 Electric vehicles (EVs)

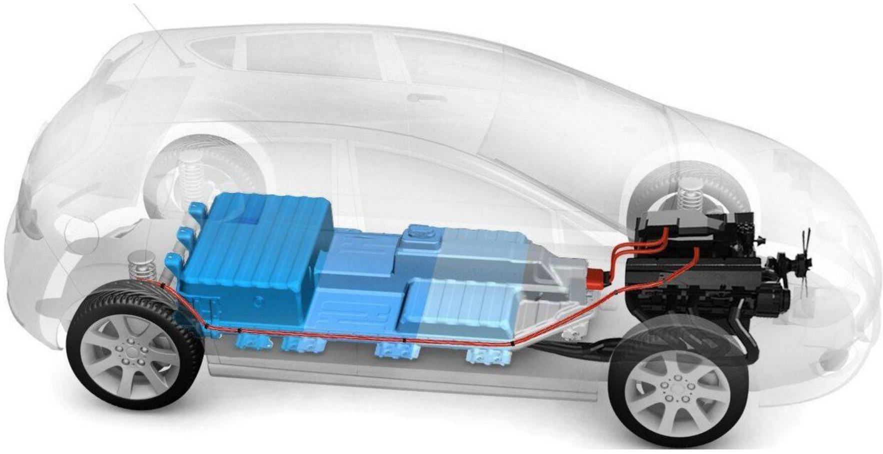

Figure 3.6 Electric vehicle battery.

While liquid fuels' price increases and climate change posing a serious threat, EVs presence start to grow. They have the ability to make the transport more sustainable and smarter, as transport is responsible for one quarter of Europe's gas emissions.

The cost gap between electric vehicles and gas models is beginning to shrink, making them a more attractive choice. As battery and motor technology advances, the cost of EVs is going to decrease and more of them is going to be imported into the grid.

More and more EV charging stations are being installed into the European countries, giving them the ability to be charged during the night of during the working hours of the people. Thus, EVs can be used as ESUs during the time they are connected to the microgrid.

3.2.6 Utility grid and net metering

The utility grid is the electrical power system designed to provide electricity to its consumers for their daily needs. It consists of generator plants, transmission lines, substations, transformers and distribution lines.

The utility grid is divided into three main processes.

- **Generation** can be divided into centralized and decentralized. Centralized generation refers to generation far from consumption like coal, nuclear, wind farms, PV parks etc. While decentralized generation apply to close to consumption units like PVs or WGs on the top of a building.
- **Transmission and distribution** process use transmission lines for electricity to be transferred from power plants to consumers. After generation, electricity voltage is stepped-up to be transferred through transmission likes with minimum losses. Before consumption, electricity voltage is stepped-down to be used.
- **Consumption** process varies, based on consumer's needs that stated in section (2.2.1).

However, the network maintains a two-way relationship with prosumers. In recent years a new concept has emerged in the energy market called net metering. Net metering is a framework under which they inject their spare produces energy by RES into the utility grid, in order to use that amount of energy in another time period. This way, the grid is used as a storage system for these customers.

Net metering presents many benefits for prosumers and for the grid. This system is easy to be implemented by prosumers giving the ability to save energy, and consequently reduce operating costs, without having to purchase an ESU. The utility grid is benefited by private distributed energy production, because it decreases the need for centralizing power plants. This way the grid's operating costs are declined.

On the other hand, with the use of net metering, prosumers who produce much more energy than needed for their energy demands are losing this energy because net metering doesn't offer excessive energy purchasing.

In this study, grouping prosumers into microgrids is proposed. Then, net metering is going to apply to the whole microgrid using the excessive energy of a group of customers. Using this approach, prosumers can meet the energy needs of a neighboring consumer, with their surplus energy, by selling it to them. So, this amount of energy that wouldn't be useful in the regular application of net metering, in the proposed application would economically benefit the power producer.

A microgrid can consist of different types of buildings, RESs and ESUs. In addition to photovoltaics and wind turbines there could be a hydroelectric system or geothermal power generation. In terms of energy storage, there could be solar thermal power plants or hydrogen energy storage. While electric vehicles could also include electric trains and buses. However, this study is limited to the use of buildings, photovoltaics, wind turbines, batteries and electric cars.

3.3 Microgrid Control

In order to control a microgrid, there is the centralized method and the decentralized method [16]. While centralized method makes use of all the system's data collectively in order to take a decision, decentralized method blindly controls a unit without any information about the other units. However, decentralized method is faster in execution time, but centralized method is much more optimal. So, a combination of these two methods is used in order to create a control system that is optimal and takes fast decisions. As shown in Figure 3.7, the microgrid control system consists of the monitor, control and optimize unit. The combination of a set of sensors and the analyzing algorithm of the extracted data, form the monitor unit. Control unit contain the processes of primary control and secondary control, while optimize unit concludes the control system by containing the tertiary control.

- **Primary control**
  In primary control takes place the voltage and frequency stabilization, the active and reactive power sharing among units and the circulation current manipulation to avoid over-current cases in the power electronic devices.
- **Secondary control** as a centralized controller, restores the microgrid voltage and frequency and compensates for the deviations caused by variations of loads or renewable sources power generation. The secondary control can also be designed to satisfy the power quality requirements.
- **Tertiary control** refers to the last step of control into the microgrid that considers load demand, energy production, weather, economic data, like hourly electricity price, in order create an hourly of daily load exchange prediction with the utility. This prediction has to secure optimal energy usage and economical savings.

A microgrid energy management system require sensors, microcontrollers and an intelligent software algorithm to operate. The control system must be able to know about the environmental conditions inside microgrid's structures, but also weather conditions. Also, it must be able to communicate with the energy provider for energy price information. Using this information, predictions can be made by the control system that can be used in the energy management process, in order to have an optimized operation of the microgrid.

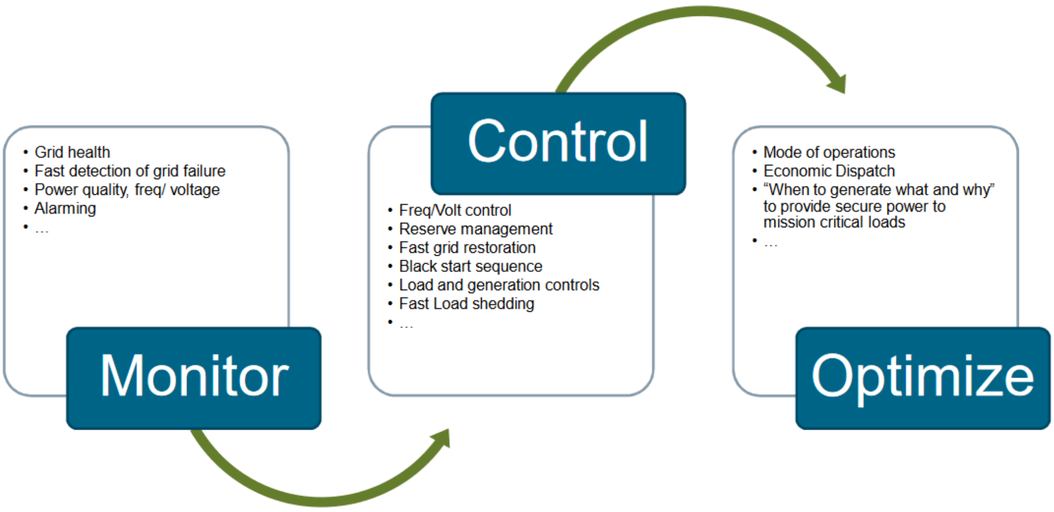

Figure 3.7 Control system of a microgrid. Source: IEEE

3.3.1 Sensors and metering devices

There are several sensors that need to be used in order to manage a microgrid. Sensors for building's load, RES energy generation, electric vehicle charging power, weather and battery power monitoring are going to be used in this study.

- **Building load monitoring**
  To monitor and get energy consumption measurements from a set of buildings, a circuit monitoring system (CMS) can be used that saves these measurements. A CMS sensor by CMS-700 system of ABB is shown in Figure 3.8 that measures up to 160 A and can be mounted to a cable. Measurement data are transmitted digitally via the CMS-bus interface from each sensor to the sensor control unit. The sensor control unit is shown in Figure 3.9, that can be connected to 96 sensors. This way, sensors can be connected to the electrical loads of each building, measuring the hourly energy consumption and giving data to the energy management system for the load demand.

Figure 3.8 CMS sensor. Source: ABB

Figure 3.9 Sensor control unit. Source: ABB

- **RESs energy generation and battery power monitoring**
  In Figure 3.10 an energy meter is shown that allows active power, voltage, current and power factor measurements. RESs and battery power can be monitored using this type of energy meters, informing the energy management system about the available energy by production and energy saved to the battery.

Figure 3.10 Energy meter. Source: ABB

- **Electric vehicle charging power** can be monitored through the electric vehicle charger. Chargers like Terra 54 by ABB, shown in Figure 3.11, offer this option of saving data about a vehicle’s charging session. Using this information of all chargers, it can be calculated the number of vehicles that are being charged during the day into the microgrid and consequently the hourly load needed.

Figure 3.11 Terra 54 CJG Fast charger. Source: ABB

- **Weather monitoring**
  A microgrid energy management system need to measure temperature, irradiation and wind conditions through the day, to be able to predict photovoltaic and wind generator energy production and also control the air-conditioning system. A weather station, like the one shown in Figure 3.12, can be used in order to monitor hourly of daily datasets of weather conditions.

Figure 3.12 VSN800 Weather station. Source: ABB

The measurements made by the sensors are stored, aiming to the creation of weather forecasts for future use of the EMS. The better and more accurate the forecasts made, the more efficient the EMS will be. This requires a good system for managing and using this data.

3.3.2 Microcontrollers and control units

As mentioned above, there is the primary, secondary and tertiary control. Each control step uses a set of control devices.

In primary control, a distributed control system (DCS) needs to be implemented in order to allow local controllers to have autonomy and make fast decisions for each unit's protection. The DCS provides the primary control of the microgrid, using power sharing between the units and local voltage control for stabilizing the operation of it. In Figure 3.13 a DCS controller is shown which can be used to control a unit of the microgrid, offering human-machine interface for easier monitoring.

Figure 3.13 AC 800M Controller by DCS system. Source: ABB

Continuing to the secondary control, an intelligent electronic device (IED) is needed to automate the control process of the primary stage. IEDs are microprocessor-based devices, able to exchange data and control signals with other devices over a communication protocol. In Figure 3.14, an IED device is presented that can be used for bidirectional or non-directional overcurrent, voltage and frequency stabilization, power based and earth-fault protection and measurement functionality.

Figure 3.14 Feeder protection and control IEC. Source: ABB

Concluding, the tertiary control step follows the monitoring and (primary and secondary) controlling step. This part of the control system, relies on the monitored and predicted data extracted by the monitoring unit and on the assumption that every microgrid component is functioning properly, based on the proper control unit operation. In this step, a small, low power microcontroller needs to be used to execute the energy management algorithm that will be used. Therefore, a Raspberry Pi Computer, shown in Figure 3.15, can be implemented to be connected with all sensor systems and controlling devices to handle their operation based on the optimal scenario that the algorithm predicts.

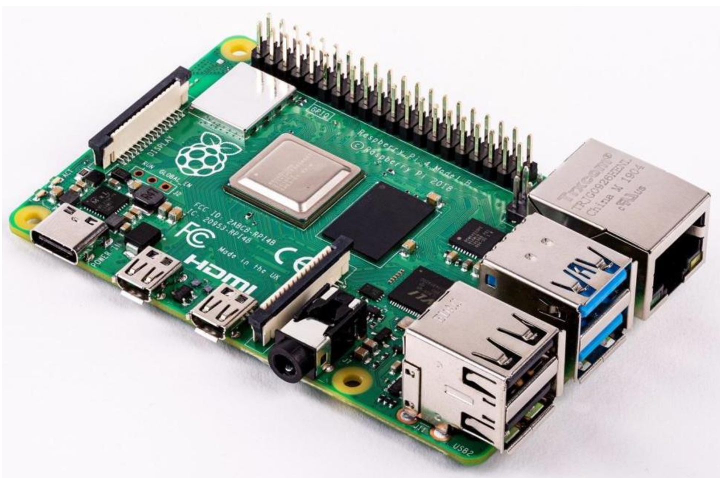

Figure 3.15 Raspberry Pi Computer

3.3.3 Optimization algorithms

In order to control such a complex system as a microgrid, a decision-making method is needed that can handle the size of this problem. Optimization is a great tool to solve this kind of problems, as the procedure of optimization focus on the minimization of maximization, though mathematical equations, of a target value. This value is calculated based on the selected solution, that got picked by a group of possible solutions.

Optimization problems consist of three main elements.

- An **Objective function** expresses the reference value calculation function that must be maximized or minimized. The calculation function of total microgrid cost or the summary of microgrid's energy usage can be used as objective function.
- A **collection of variables** which values are being manipulated in order to optimize the objective function.
- A **set of constraints** is needed that limits the manipulation of variables and other objective function values, so they are into the given margin.

Several optimization methods are used for problem solving that differ in the solution approach but also the ability to solve complex problems.

- **Linear programming** focuses on the case in which the objective function is linear and the constraints are expressed using linear equalities and inequalities.
- **Geometric programming** is the method, in which the objective and inequality constraints are expressed as posynomials and the equality constraints as monomials.
- **Integer programming** is similar to linear programming but in this case some or all variables can take only integer values.
- **Quadratic programming** uses constraints expressed in linear equalities and inequalities, but the objective function is allowed to have quadratic terms.
- **Non-linear programming** allows the objective function or the constraints to contain non-linear parts.
- **Stochastic optimization** studies the case in which some of the constraints or parameters are produced with the use of random function measurements or random inputs.
  - Particle swarm optimization (PSO) algorithm is a stochastic optimization technique based on swarm, which was proposed by Eberhart and Kennedy (1995). PSO algorithm was inspired by birds' and fish's social behavior and is based on behavior readjustment, according to the learning experience of its own or other members. PSO's detailed description is given in the next chapter.
- **Dynamic programming** studies the case in which the optimization strategy is based on splitting the problem into smaller sub-problems.
- **Constraint programming** uses a constant objective function, but relations between variables are stated in the form of constraints.
- **Heuristics** are algorithms that doesn't guarantee that they are going to find the optimal solution, but they are very useful in particle situations. Some well-known heuristics are:
  - Reactive search optimization (RSO) advocates the integration of machine learning techniques into search heuristics for solving complex optimization problems. Its strength lies in the introduction of high-level skills often associated to the human brain,

such as learning from the past experience, learning on the job, rapid analysis of alternatives, ability to cope with incomplete information, quick adaptation to new situations and events.

- Hill climbing algorithm belongs to the family of local search, but using the random restart feature, can be categorized into a heuristic algorithm. It is an iterative algorithm that starts with an arbitrary solution to a problem, then attempts to find a better solution by making an incremental change to the solution.
- Genetic algorithms (GA) are used to generate high quality solutions for optimization problems using bio-inspired operators like mutations, crossover and selection.

4. PROBLEM FORMULATION

4.1 Microgrid Of Large Building Prosumers

The structure of the microgrid of large building prosumers examined in this thesis is shown in Figure 4.1.

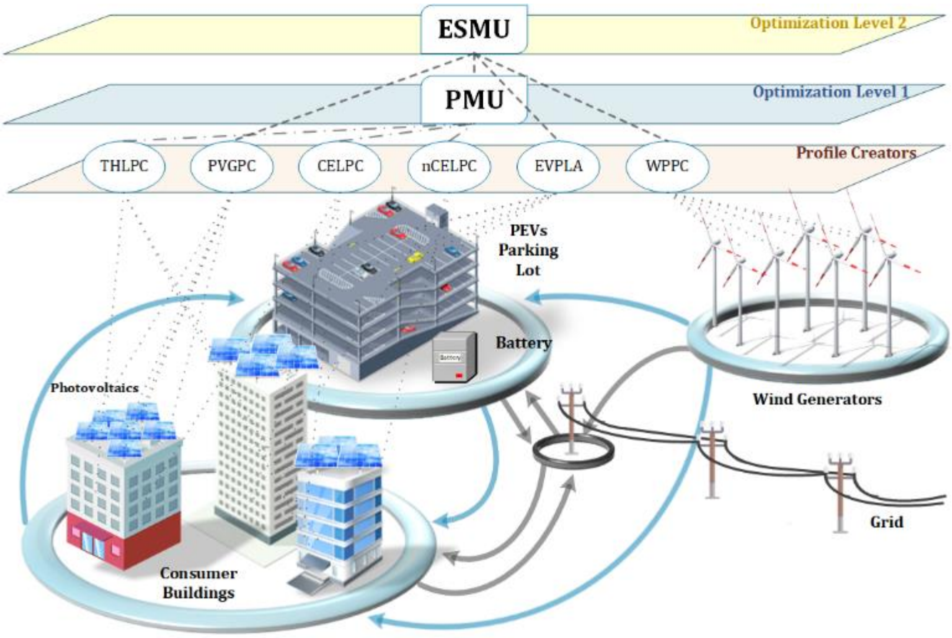

Figure 4.1 Real-world deployment of the proposed microgrid energy management system

It consists of a group of buildings powered by the electric grid, renewable energy sources and energy storage units. Both the electrical and thermal loads of the buildings are considered in our analysis. Regarding the energy storage facilities, a conventional battery and a cluster of electric cars plugged to the charging stations of the buildings of the microgrid are considered. The examined system of building prosumers also comprises photovoltaics on the roofs of the buildings and wind turbines placed nearby or far from them. Even in case that renewable energy sources are located away from the group of buildings they can be considered part of the microgrid if they are under the same ownership with the buildings. In this way, virtual prosumers can be formed but more advanced communication and control systems would be required.

The hierarchical multi-agent system [3-5,12,13] shown in Figure 4.1 was appropriately designed to optimally schedule the operation of the supervised microgrid of building prosumers. It consists of different types of agents assigned with specific functions described next. Specifically, the developed types of agents are: 1) The Load Profile Creators are responsible for the estimation of the profile of a specific type of load within the optimization period, 2) The Power Management Unit and Energy Management Unit execute optimization algorithms to determine the optimal operation of the HVAC (Heat, Ventilation and Cooling), the electrical systems and the energy trading with the network via suitable regulation of the energy storage devices, respectively. Next, the function of each agent type is briefly described while their models are given in the next section.

Load Profile Creators: Thermal Load Profile Creator (THLPC), Critical Electrical Load Profile Creator (CELPC) and non-Critical Electrical Load Profile Creator (nCELPC) belong in this category of agents. They are responsible to estimate the profiles of thermal and electrical loads (critical and non-critical) taking into account the forecasted human activity in each building thermal zone. More specifically, these forecasts are based on the number of the people expected to have activities in each building thermal zone as well as the use of a number of electrical appliances by them within the optimization period. Photovoltaic Generation Profile Creator (PVGPC) and Wind Power Profile Creator (WPPC) also belong to same type of agents. They are assigned with the estimation of the respective power generation profiles based on weather forecast. Finally, the Electric Vehicle Parking Lot Profile Aggregator (EVPLA) estimates an equivalent battery model for the plug-in electric vehicles (PEVs) expected to be hosted in the group of buildings based on forecasts of their connection and dwell times, their initial state of charge and their technical characteristics.

Power Management Unit (PMU): It optimizes the operation of each building thermal zones HVAC system, based on the ambient temperature and electricity price forecasts and the electrical load profiles received by CELPCs and nCELPCs. The result is the optimal electric power demand of the HVAC systems, the optimal time shifting of the non-critical electrical loads of every thermal zone so that the respective energy cost is minimized and all operational and technical constraints of the thermal-electric system e.g. indoor temperature upper and lower levels, min-max power of HVACs, are satisfied.

Energy Storage Management Unit (*ESMU*): It performs the last step of the optimization of the microgrid. It uses as input the outputs of the PMUs, the forecasted RESs energy production and electricity price to estimate the optimal profile of the power exchanged by the cluster of PEVs and the battery with the electrical grid. The main target of ESMU is the minimization of the operation cost of the whole system with the full satisfaction of the constraints of the energy storage systems.

4.2 Microgrid Components' Models

In this section, the models of the thermal and the electrical systems of the buildings, the battery, the cluster of PEVs hosted by the microgrid of buildings, the wind generators and the photovoltaics are presented.

4.2.1 Building Thermal Modeling

In this study, each building is divided into thermal zones. More specifically, the zth floor corresponds to the zth thermal zone (subscript z denotes the zth thermal zone of the building) modeled by the following equations [12].

$$\rho_z \cdot C_z \cdot V_z \cdot \frac{dT_z}{dt} = Q_{wall,z} + Q_{win,z} + Q_{in,z} + Q_{sw,z} + Q_{sg,z} - Q_{HVAC,z} + Q_{cp,z} \quad (1)$$

with

$$Q_{wall,z} = U_{wall,z} \cdot F_{wall,z} \cdot \left(\hat{T}_{amb} - T_z\right) \quad (2)$$

$$Q_{win,z} = U_{win,z} \cdot F_{win,z} \cdot (\hat{T}_{amb} - T_z) \quad (3)$$

$$Q_{sw,z} = \alpha_{w,z} \cdot R_{se,z} \cdot U_{wall,z} \cdot F_{wall,z} \cdot I_{T,z} \quad (4)$$

$$Q_{sg,z} = \tau_{win,z} \cdot SC_z \cdot F_{win,z} \cdot I_{T,z} \quad (5)$$

$$Q_{cp,z} = \sum_{k \in NZ} U_{fl,z} \cdot F_{fl,z} \cdot (T_k - T_z) \quad (6)$$

$$Q_{in,z} = \hat{N}_{P,z} \cdot \sum_{j \epsilon J_{th}} N_{j,z} \cdot Q_{j,z} \quad (7)$$

$$I_{T,z} = \hat{I}_b \cdot R_b \cdot \hat{I}_d \cdot \left(\frac{1 + cos\beta_z}{2}\right) + \hat{I} \cdot \rho_g \cdot \left(\frac{1 - cos\beta_z}{2}\right) \quad (8)$$

$$R_b = \frac{cos\theta}{cos\theta_Z} \quad (9)$$

$$P_{HVA\,C,z} = \frac{Q_{HVAC,z}}{COP} \quad (10)$$

$$\underline{P}_{HVAC,z} \leq P_{HVAC,z} \leq \overline{P}_{HVAC,z} \quad (11)$$

$$\underline{T}_z \leq T_z \leq \overline{T}_z \quad (12)$$

$$T_z(0) = T_z(T) \quad (13)$$

Where, ρ_z, C_z and V_z represent the density, specific heat capacity and volume of the air in the thermal zone, $Q_{wall,z}$ is heat transfer through the external walls , $Q_{win,z}$ is heat transfer through the windows, $Q_{sw,z}$ is heat gain due to solar radiation on the external walls, $Q_{sg,z}$ is heat gain due to solar radiation on the windows, $Q_{cp,z}$ is heat exchanged by adjacent thermal zones, $Q_{in,z}$ is heat gain by the internal thermal loads $Q_{j,z}$ of a number ($N_{j,z}$) of jth type loads (such as humans, screens, lamps, etc.), $\hat{N}_{P,z}$ is the forecasted number of people being in the zth thermal zone, Q_{HVAC} is the cooling power of the HVAC, $P_{EC,z}$ and E_{EC} are the electric power and energy consumed by the HVAC and COP is its performance coefficient . J_Z denotes the set of thermal loads within the zth thermal zone, $Z = \{z_1, z_2, \dots, z_\mathrm{n}\}$ the set comprising the thermal zones of a building and $Nz = \{nz_1, nz_2, \dots, nz_\mathrm{n}\}$ the set comprising the neighboring zones of the zth thermal zone.

Moreover, $U_{wall,z}$, $U_{win,z}$ and $U_{fl,z}$ are the heat transfer coefficients of the wall, window and floor respectively. $F_{wall,z}$, $F_{win,z}$ and $F_{fl,z}$ are the total wall, window and floor surface of the thermal zone, $\hat{T}_{amb}$ is the ambient temperature, T_z and T_{nz} are the indoor current zone and neighboring zone temperature respectively, $\alpha_{w,z}$ is the absorbance coefficient of the external wall surface , $R_{se,z}$ is the external surface heat resistance, τ_{win} is the heat transmission coefficient of window glasses and SC_z is window shading coefficient. $\hat{I}_b$, $\hat{I}_d$ and $\hat{I}$ are the beam, diffuse and total radiation on horizontal surface respectively; ρ_g is the ground reflectance; θ and θ_Z are incidence and zenith angles; β_z the surface slope.

$\underline{P}_{HVAC,z}$ and $\overline{P}_{HVAC,z}$ are the lower and upper limits of the electric power consumed by HVAC, $\underline{T}_z$ and $\overline{T}_z$ the lower and upper limits of the zth zone's internal temperature respectively. T denotes the optimization period.

4.2.2 Modeling of Building Electrical Loads

In order to estimate the electric power consumption human activity has to be predicted for each building thermal zone during the optimization period together with the number and type of electrical devices used by them. The power consumed by the electric loads of the zth building thermal zone is calculated as in the following.

$$P_{el.z} = \widehat{N_{P,z}} \cdot \sum_{j \in J_{el}} N_{j,z} \cdot P_{j,z} \qquad (14)$$

Where $P_{el,z}$ is the total power of the electrical loads within the zth thermal zone respectively, $N_{j,z}$ is the number of electrical appliances of jth type and $P_{j,z}$ is the electrical power consumed by this type of electrical appliance. Finally, $J_{el}$the set of electrical appliances used by a person.

Buildings comprise critical electrical loads which are not flexible in their operation e.g. lighting, computers etc. and non-critical loads that can be adjusted and shifted in time. e.g. smart vacuum cleaners, dish washers, water heaters etc. In this work, the electric power consumption of the non-critical electrical loads, P_{nCr}, is modeled as a constant proportion (n_{nCr}) of the electrical loads as in the following.

$$P_{nCr} = n_{nCr} \cdot \sum_{z} P_{el,z} \qquad (15)$$

Non-critical loads can be optimally shifted in time according to (16)-(18).

$$P^*_{nCr}(t) = \begin{cases} n_{sh}(t) \cdot P_{nCr}(t) & , \underline{T}_{sh} \leq t \leq \overline{T}_{sh} \\ P_{nCr}(t) & , otherwise \end{cases} \qquad (16)$$

$$\underline{n}_{sh} \leq n_{sh} \leq \overline{n}_{sh} \qquad (17)$$

$$\sum_{t=\underline{T}_{sh}}^{\overline{T}_{sh}} P_{nCr}(t) \cdot \Delta t = \sum_{t=\underline{T}_{sh}}^{\overline{T}_{sh}} P^*_{nCr}(t) \cdot \Delta t \qquad , \forall z \qquad (18)$$

Where, P_{nCr}^{*} is the optimal power consumed by the non-critical electrical loads , n_{sh} is a coefficient calculated by the optimization algorithm executed by the PMU in order to optimally adjust the non-critical loads, $\underline{T}_{sh}$ and $\overline{T}_{sh}$ denote the beginning and the end of the time period where the non-critical loads can be adjusted or shifted in time.

4.2.3 Photovoltaic Generator Modeling

Photovoltaics (PVs) are assumed to be placed on the roofs of the buildings. The electric power generated by the PVs is calculated as it follows.

$$\hat{P}_{PV} = n_{PV} \cdot P_{PV,N} \cdot \frac{\hat{G}}{G_{ref}} \cdot \left[1 + K_t \left(\left(\hat{T}_{amb} + 0.0256 \cdot \hat{G}\right) - T_{ref}\right)\right] \quad (19)$$

Where $P_{PV,N}$ is the nominal power of the PV generator, $\hat{G}$ is the forecasted solar radiation, G_{ref} (1000 W/m^2) is the reference solar radiation, K_t is a constant equal to $-0.037\ °C^{-1}$ and T_{ref} (25 °C) the panel temperature in standard test conditions , n_{PV} is the performance coefficient of the PV power converter.

4.2.4 Wind Generator Modeling

The examined microgrid of buildings comprises a number of small wind generators (WGs) that can be mounted on the buildings or belong to a small wind farm operated by the microgrid. The power generation of the WGs is calculated in the following.

$$\hat{P}_{WG} = n_{WG} \cdot \begin{cases} 0, & \hat{V} < V_{cut-in}, \hat{V} > V_{cut-out} \\ \hat{V}^3 \left(\frac{P_{WG,N}}{V_N^3 - V_{cut-in}^3}\right) - P_{WG,N} \left(\frac{V_{cut-in}^3}{V_N^3 - V_{cut-in}^3}\right) & , V_{cut-in} \le \hat{V} < V_N \\ P_{WG,N} & , V_N \le \hat{V} < V_{cut-out} \end{cases} \quad (20)$$

Where, n_{WG} is the performance coefficient of the WG power converter, $\hat{V}$ is the forecasted wind velocity, V_N is the nominal wind velocity of the WG, V_{cut-in} ($V_{cut-out}$) is the cut-in (cut-off) wind velocity, and $P_{WG,N}$ is the nominal electric power of the WG.

4.2.5 Building Energy Storage System Modeling

Let us denote with $P_{g,ESS}$ the power that the energy storage system (ESS) converter exchanges with the network.

Then the ESS power is calculated as:

$$P_{ESS} = \begin{cases} P_{g,ESS} \cdot n_{ch} & , P_{g,ESS} > 0 \\ \frac{P_{g,ESS}}{n_{dch}} & , P_{g,ESS} \le 0 \end{cases} \quad (21)$$

n_{ch} and n_{dch} are the performance coefficients of the ESS power converter while charging or discharging, respectively.

The ESS state of charge (SoC) representing the stored energy is then calculated as in the following.

$$SOC_{ESS}(t) = SOC_{ESS}(t - \Delta t) + P_{ESS}(t) \cdot \Delta t \quad \forall\, t \in T \quad (22)$$

Moreover, the ESS operation is subject to the following constraints.

$$\underline{P}_{g,ESS} < P_{g,ESS} < \overline{P}_{g,\mathrm{ESS}} \quad (23)$$

$$\underline{SOC}_{ESS} < SOC_{ESS} < \overline{SOC}_{ESS} \quad (24)$$

$$SOC_{ESS}(0) = SOC_{ESS}(\mathrm{T}) \quad (25)$$

Where $\underline{P}_{g,ESS}$ and $\overline{P}_{g,ESS}$ are the lower and upper limits of ESS power, $\underline{SOC}_{ESS}$ and $\overline{SOC}_{ESS}$ are the lower and upper limits of ESS SoC, T denotes the end of the ESS operation period.

In case that the microgrid should operate autonomously within a specific time period e.g. electric grid power supply outage, then the following supplementary constraints should be applied.

$$\underline{SOC}_{ESS}(t') \geq \sum_{t=t'}^{\overline{T}_{aut}} \sum_{b} \sum_{z} \left(n_{aut} \cdot \left(P_{el,b,z}(t) + P_{HVA\,C,b,z}(t)\right) - \hat{P}_{PV}(t) - \hat{P}_{WG}(t)\right) \cdot \Delta t$$

$$\forall t' \epsilon [\underline{T}_{aut}\ \overline{T}_{aut}], b \in B, z \in Z \quad (26)$$

$$\sum_{b} \sum_{z} n_{aut} \cdot \left(P_{el,b,z}(t) + P_{HVA\,C,b,z}(t)\right) - \hat{P}_{PV}(t) - \hat{P}_{WG}(t) \leq \overline{P}_{g,\mathrm{ESS}}$$

$$\forall\, t \epsilon [\underline{T}_{aut}\ \overline{T}_{aut}], b \in B, z \in Z \quad (27)$$

Where, B is the set comprising the buildings of the microgrid, Z is the set of the building thermal zones, $[\underline{T}_{aut}\ \overline{T}_{aut}]$ denotes the time period within which the microgrid should operate autonomously.

4.2.6 Electrical Vehicle Parking Battery Modeling

Next, an equivalent battery model for the cluster of PEVs hosted by the microgrid is developed. The main target of the following analysis is to obtain the dynamic upper and lower limits of the SoC and the active power of the equivalent battery of the cluster of PEVs in order to optimally schedule the power they will exchange with the network.

Let us denote with $P_{g,EVPB}$ the power exchanged by the equivalent battery of the EVs parking and the grid. Then the equivalent battery charging (discharging) power and its SoC are calculated in the following.

$$P_{EVPB} = \begin{cases} P_{g,EVPB} \cdot n_{ch} & , P_{g,EVPB} > 0 \\ \dfrac{P_{g,EVPB}}{n_{dch}} & , P_{g,EVPB} \leq 0 \end{cases} \quad (28)$$

$$SOC_{EVPB}(t) = SOC_{EVPB}(t - \Delta t) + SOC_d(t) + P_{g,EVPB}(t) \cdot \Delta t \quad (29)$$

SOC_d denotes the dynamic change of SOC_{EVPB} due to the plugging or unplugging of EVs from the network. It is calculated in (30).

$$SOC_d(t) = \sum_i \sum_{t'=0}^{t} st(i,t') \cdot \{SOC_i(t_{0,i}) - SOC_i(t_{f,i})\} \quad (30)$$

Where, $t_{0,i}$ is the time the ith PEV is connected (disconnected) to (from) the electric network, $st(i,t)$ is a binary variable that equals 1 if $t = t_{0,i}$ or $t = t_{f,i}$ otherwise it equals 0.

Moreover, the equivalent battery should satisfy the following constraints.

$$\underline{P}_{g,EVPB} < P_{g,EVPB} < \overline{P}_{g,EVPB} \quad (31)$$

$$SOC_{l,EVPB} < SOC_{EVPB} < SOC_{h,EVPB} \quad (32)$$

with

$$SOC_{h,EVPB} = \sum_i SOC_{h,i} \quad (33)$$

$$SOC_{l,EVPB} = \sum_i SOC_{l,i} \quad (34)$$

$$SOC_{h,i}(t) = \begin{cases} \overline{SOC}_i(t) & , t < t_{h,i} \\ \overline{SOC}_i(t) - \overline{P}_i \cdot (t - t_{h,i}) & , t > t_{h,i} \end{cases} \quad (35)$$

$$SOC_{l,i}(t) = \begin{cases} \underline{SOC_i}(t) & , t < t_{l,i} \\ \underline{SOC_i}(t) + \overline{P}_i \cdot (t - t_{l,i}) & , t > t_{l,i} \end{cases} \quad (36)$$

$$\overline{P}_{g,EVPB}(t) = \sum_i \begin{cases} \overline{P}_i(t) & , t_{0,i} < t < t_{f,i} \\ 0 & , otherwise \end{cases} \quad (37)$$

$$\underline{P}_{g,EVPB} = -\overline{P}_{g,EVPB} \quad (38)$$

$t_{h,i}$, $t_{l,i}$ are calculated as,

$$t_{h,i} = t_{f,i} - \frac{\overline{SOC}_i - SOC_{tg,i}}{\overline{P}_c} \qquad (39)$$

$$t_{l,i} = t_{f,i} - \frac{SOC_{tg,i} - \underline{SOC}_i}{\overline{P}_i} \qquad (40)$$

Where, $\underline{P}_{g,EVPB}$ and $\overline{P}_{g,EVPB}$ are the lower and upper limits of the power of the equivalent battery, $SOC_{h,EVPB}$ and $SOC_{l,EVPB}$ refer to the upper and lower limits of the SOC (in kWh) of the equivalent battery, $SOC_{h,i}$ and $SOC_{l,i}$ are the upper and lower limits of the SOC of the ith PEV's battery , $\overline{P}_i$ the maximum power of the ith PEV, $\underline{SOC}_i$ and $\overline{SOC}_i$ are the minimum and maximum values of the ith PEV's SoC, $SOC_{tg,i}$ the target SoC of the ith PEV when unplugged from the network $SOC_{0,\mathrm{i}}$ the initial SOC of the ith PEV, $t_{0,\mathrm{i}}$ and $t_{f,i}$ are the plugging and unplugging times of a PEV, respectively.

4.3 Optimization

4.3.1 Particle swarm optimization algorithm (PSO)

Just like evolutionary algorithms, PSO uses a swarm, to simultaneous search large region in the solution space of the optimized objective function, but also studies an artificial system with life characteristics.

PSO is an optimization algorithm, that operate a searching process using a swarm. Each individual of the swarm is called a particle that can be a possible solution to the optimization problem in *D*-dimensional search space. Every particle has information about its own optimal position and velocity. Then PSO, using this information from all of the particles, calculates the optimal position of the swarm and adjusts all of the velocities of each dimension. Due to the change of the velocity in every dimension, particles use this to compute their new position. Particles change their states constantly in the multi-dimensional search space, until they reach balance or optimal state, or beyond the calculating limits. The state of a swarm is calculated with the use of an objective function, connecting all the problem dimensions. Many empirical evidences have showed that this algorithm is an effective optimization tool. Flowchart of the PSO algorithm is shown in Figure 4.2.

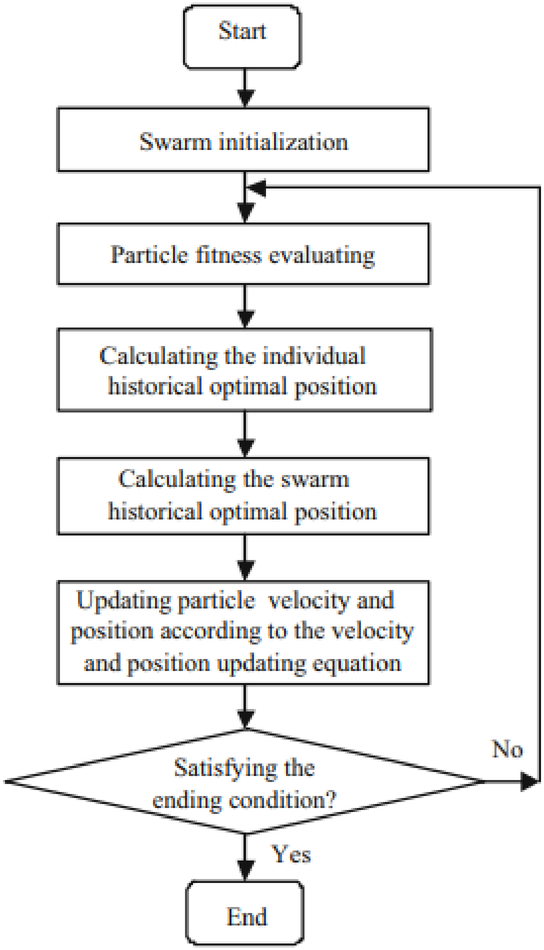

Figure 4.2 Flowchart of the particle swarm optimization algorithm

Inertia weight ω, learning factors c1 and c2, speed limits V_{max}, position limits X_{max}, swarm size and the initial swarm are several important parameters in PSO algorithm. These parameters are used to give a direction to the algorithm, in order to have the smallest execution time and most optimal solution possible.

- **Inertia weight** is used to balance the global search and the local search. Bigger inertia weight is tended to global search while the smaller inertia weight is tended to local search, so the value of inertia weight should gradually reduce within time.
- **Learning factors c1 and c2** represent the weights of the stochastic acceleration terms that pull each particle toward pBest (particle best optimization value) and gBest (global best optimization value). In many cases, c1 and c2 are set to 2.0 which make the search to cover the region centered in pBest and gBest.
- **Speed limit** represents the constraint that a particle has in order to control the search ability of it.
- **Position limits**
  Positions of the particles can be constrained by a maximum position X_{max} that can avoid particles flying out of the physical solution space.

- **Population size** refers to the swarm size, or particle population, that is going to be used to solve a problem. Common selection is 20–50, but in some cases larger population is used to meet the special needs.
- **Initialization of the population** is also a very important problem. Generally, the initial population is randomly generated, but there are also many intelligent population initialization methods that can be used.

4.3.2 Power Management Unit

The first stage of optimization is performed in PMU where the operation cost of the HVAC system and non-critical electrical loads is minimized at building level. At the same time all operation and technical constraints are satisfied. The formulation of the examined optimization problem is provided next.

$$\min_{\substack{P^*_{HVAC,z},\\ P^*_{nCr}}} \left\{ \sum_t \sum_z \left(P^*_{HVAC,z}(t) + P^*_{nCr}(t) \right) \cdot EP(t) \cdot \Delta t \right\} \qquad (41)$$

S.t. (11)-(13), (17)-(18)

Where, $P^*_{HVAC,z}$ is the optimal HVAC electrical power consumption at the zth thermal zone of the building, P^*_{nCr} the optimized electrical power by the non-critical loads and EP the electricity price.

Particle swarm optimization (PSO) method was used to solve the above problem. The structure of a particle of the swarm is shown in Figure 4.3. The first section of the particle comprises the HVAC electrical power consumption over each time interval and for all building thermal zones. The second one comprises the adjustment coefficients of the non-critical loads of the building.

In order to apply the PSO method, the augmented objective function provided in (41) was used. Except from the total operation cost of the HVAC and the non-crtical loads it comprises a number of penalty factors in order to take into account the technical and operation constraints of the system.

$$\min_{\substack{P^*_{HVAC,z},\\ P^*_{nCr}}} \left\{ \sum_t \sum_z \left(P^*_{HVAC,z}(t) + P^*_{nCr}(t) \right) \cdot EP(t) \cdot \Delta t + \sum_p P_{PMU,p} \right\} \quad (42)$$

With,

$$P_{PMU,1} = \begin{cases} \left| \max_z\{P^*_{HVAC,z}\} - \overline{P}_{HVAC,z} \right| \cdot K_p \;, \max_z\{P^*_{HVAC,z}\} > \overline{P}_{HVAC,z} \\ \left| \min_z\{P^*_{HVAC,z}\} - \underline{P}_{HVAC,z} \right| \cdot K_p \;, \min_z\{P^*_{HVAC,z}\} < \underline{P}_{HVAC,z} \\ 0, \; otherwise \end{cases} \quad (43)$$

$$P_{PMU,2} = \begin{cases} \left| \max_z\{T_z\} - \overline{T}_z \right| \cdot K_p \;, \max_z\{T_z\} > \overline{T}_z \\ \left| \min_z\{T_z\} - \underline{T}_z \right| \cdot K_p \;, \min_z\{T_z\} < \underline{T}_z \\ 0, \; otherwise \end{cases} \quad (44)$$

$$P_{PMU,3} = |\, T_z(0) - T_z(T) \,| \cdot K_p \qquad (45)$$

$$P_{PMU,4} = \begin{cases} |\max\{n_{sh}\} - \overline{n}_{sh}| \cdot K_p, & \max\{n_{sh}\} > \overline{n}_{sh} \\ |\min\{n_{sh}\} - \underline{n}_{sh}| \cdot K_p, & \min\{n_{sh}\} < \underline{n}_{sh} \\ 0, & otherwise \end{cases} \qquad (46)$$

K_p is a large constant that provokes suitable increase of the augmented objective function when the constraints are violated.

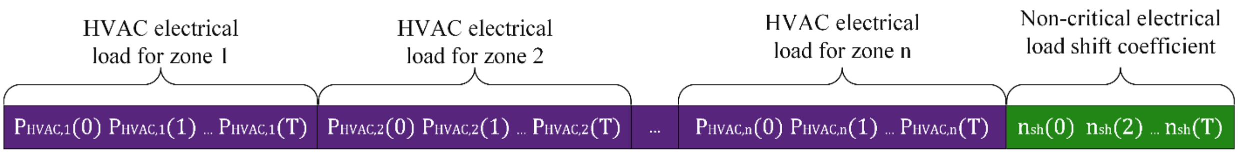

Figure 4.3 Particle structure for PSO in PMU

4.3.3 Energy Storage Management Unit

The second stage of optimization is performed in ESMU where the cost of the total electric power exchanged by the building microgrid and the grid is minimized by optimally scheduling the operation of the ESS and the EV parking lot. At the same time all respective operation and technical constraints are satisfied. The formulation of the examined optimization problem is provided next.

$$\min_{P^*_{g,ESS},\, P^*_{g,EVPB}} \left\{ \sum_t \left(\begin{array}{c} P^*_{g,ESS}(t) + P^*_{g,EVPB}(t) - \hat{P}_{PV}(t) - \hat{P}_{WG}(t) \\ + \sum_b \sum_z P^*_{HVAC,b,z}(t) + P_{el,b,z}(t) + P^*_{nCr,b}(t) \end{array} \right) \cdot EP(t) \cdot \Delta t \right\} \quad (47)$$

S.t. (23)-(27), (31)- (32)

Where, $P^*_{g,ESS}$ and $P^*_{g,EVPB}$ are the optimized powers of the ESS of the microgrid and the EV parking lot, respectively,

The structure of a particle of the swarm is shown in Figure 4.4. The first section of the particle comprises the building ESS electrical power over each time interval of the optimization period. The second one comprises the respective electric power exchanged by the EV parking lot and the electric grid.

In order to apply the PSO method, the augmented objective function provided in (47) was used.

$$\min_{P^*_{g,bat},\, P^*_{g,EVPB}} \left\{ \sum_t \left(\begin{array}{c} P^*_{g,ESS}(t) + P^*_{g,EVPB}(t) - \hat{P}_{PV}(t) - \hat{P}_{WG}(t) \\ + \sum_b \sum_z P^*_{HVAC,b,z}(t) + P_{el,b,z}(t) + P^*_{nCr,b}(t) \end{array} \right) \cdot EP(t) \cdot \Delta t + \sum_p P_{ESMU,p} \right\} \quad (48)$$

With,

$$P_{ESMU,1} = \begin{cases} \left|\max\{P_{g,ESS}^{*}\} - \overline{P}_{g,\mathrm{ESS}}\right| \cdot K_p, & \max\{P_{g,ESS}^{*}\} > \overline{P}_{g,\mathrm{ESS}} \\ \left|\min\{P_{g,ESS}^{*}\} - \underline{P}_{g,ESS}\right| \cdot K_p, & \min\{P_{g,ESS}^{*}\} < \underline{P}_{g,\mathrm{ESS}} \end{cases} \quad (49)$$

$$P_{ESMU,3} = \begin{cases} \left|\max\{SOC_{ESS}\} - \overline{SOC}_{ESS}\right| \cdot K_p, & \max\{SOC_{ESS}\} > \overline{SOC}_{ESS} \\ \left|\min\{SOC_{ESS}\} - \underline{SOC}_{ESS}\right| \cdot K_p, & \min\{SOC_{ESS}\} < \underline{SOC}_{ESS} \end{cases} \quad (50)$$

$$P_{ESMU,4} = |SOC_{bat}(0) - SOC_{bat}(T)| \cdot K_p \quad (51)$$

$$P_{ESMU,5} = \begin{cases} \left|\max\{P_{g,EVPB}^{*}\} - \overline{P}_{g,EVPB}\right| \cdot K_p, & \max\{P_{g,EVPB}^{*}\} > \overline{P}_{g,EVPB} \\ \left|\min\{P_{g,EVPB}^{*}\} - \underline{P}_{g,EVPB}\right| \cdot K_p, & \min\{P_{g,EVPB}^{*}\} < \underline{P}_{g,EVPB} \end{cases} \quad (52)$$

$$P_{ESMU,7} = \begin{cases} \left|\max\{SOC_{EVPB}\} - SOC_{h,EVPB}\right| \cdot K_{pn}, & \max\{SOC_{EVPB}\} > SOC_{h,EVPB} \\ \left|\min\{SOC_{EVPB}\} - SOC_{l,EVPB}\right| \cdot K_{pn}, & \min\{SOC_{EVPB}\} < SOC_{l,EVPB} \end{cases} \quad (53)$$

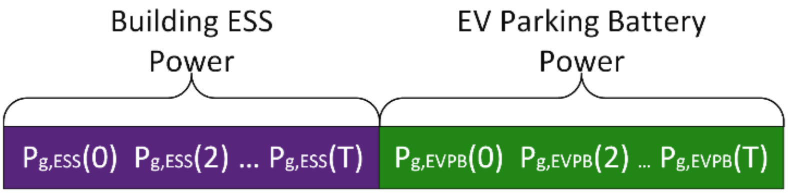

Figure 4.4 Particle structure for PSO in ESMU

4.4 Algorithm Overview

In Figure 4.5, the flowchart of the proposed EMS for the microgrid of building prosumers is shown. First, forecasts for the number of people, temperature, weather, electricity price, PEV's connection and dwell times, PEV's initial SoC and technical characteristics are are done for the next 24-hour period.

THLPC, CELPC, nCELPC, PVGPC and WPPC, exploit these forecasts to estimate the optimal profiles of building thermal and electrical loads, photovoltaic and wind power generation. Moreover, EVPLA estimates an equivalent battery model for the PEVs expected to be hosted in the group of buildings.

In Optimization Level 1, PMU is used for every building of the microgrid to optimize the operation of its HVAC and non-critical electrical loads. PMU relies its operation on the profiles created in the previous step of the algorithm.

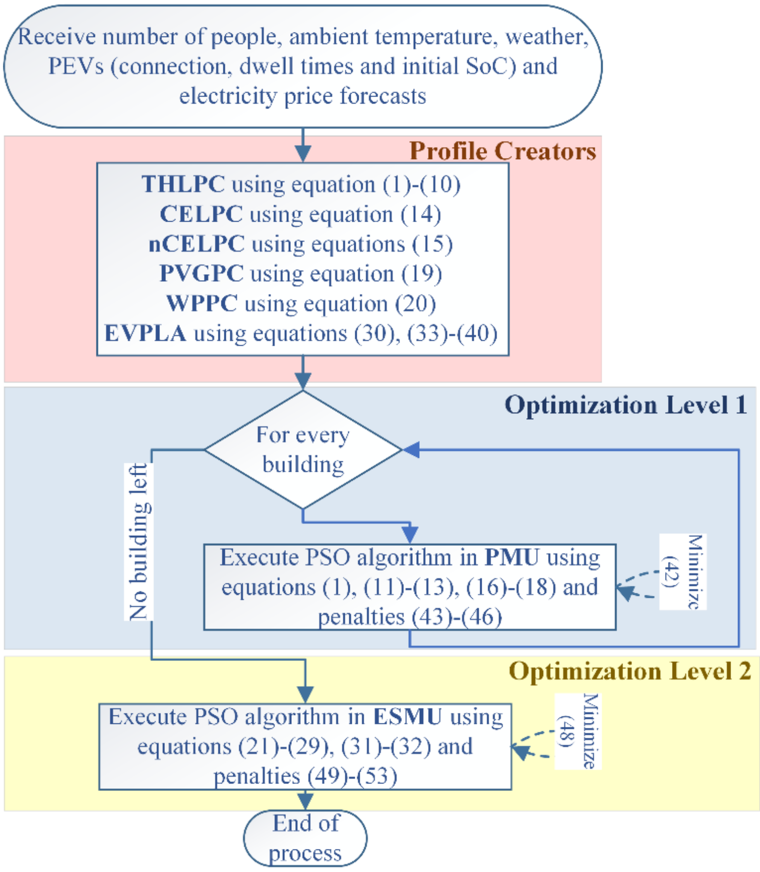

Figure 4.5 Flowchart of the proposed microgrid energy management system algorithm

In Optimization Level 2, receives the optimal electric power consumption profiles from PMU the power generation profiles for WGs and PVs and deploys the optimal power profiles for the ESS of the microgrid and the equivalent battery of the EV parking lots.

5. RESULTS

In this chapter, the case study and the results for a number of scenarios are presented, where the proposed energy management system was applied. The main goal is to prove that by implementing the described EMS, all the microgrid's energy needs and operation constraints are met. While, the total operating cost is minimized. The scenarios are used to evaluate the performance of the proposed algorithm. In order to compare the results between these different cases, the power consumed or generated by every microgrid component is presented. Also, microgrid operation cost is obtained for each scenario, to estimate the resulting cost savings.

5.1 Case Study

The Microgrid shown in Figure 5.1, is used to verify the effectiveness of the developed energy management algorithm. The parameters of the microgrid are presented in Table 5.1. Moreover, the electricity price, ambient temperature, sun radiation and wind velocity forecasts of 15th of July 2019 are utilized.

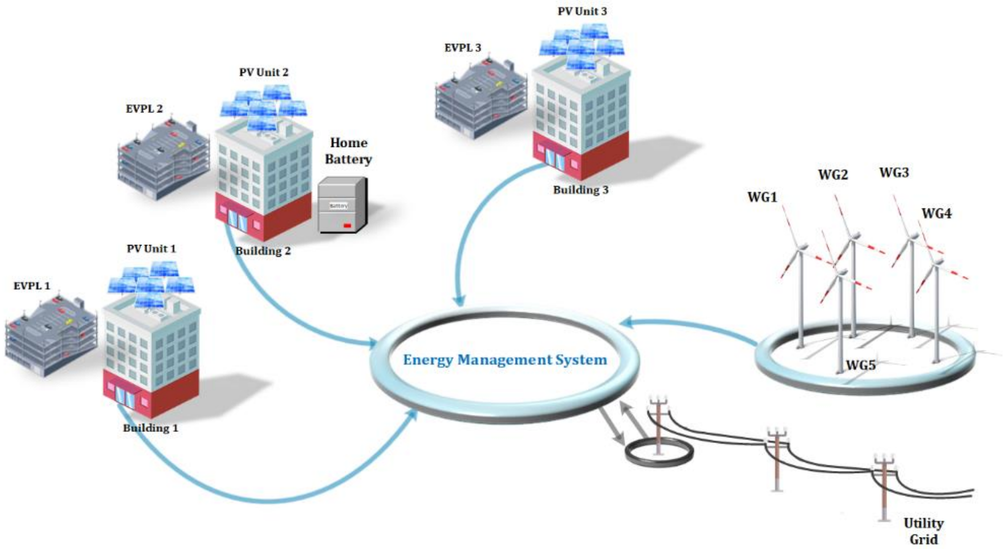

Figure 5.1 Microgrid Structure

Table 5.1 Microgrid Parameters

Building parameters		Building 1		Building 2		Building 3	
B	3	Z (Floors)	3	Z (Floors)	4	Z (Floors)	2

Floor parameters					
ρ_z (kg/m^3)	1.2	$F_{fl,z}$ (m^2)	800	ρ_g	0.2
C_z(J/ (kg·°C))	1000	$\alpha_{w,z}$	18.63	β_z	90°
V_z(m^3)	4000	$R_{se,z}$ (m^2 ·°C)/W	0.04	θ	11.9°
				COP	3.5
$U_{wall,z}$ (W/ (m^2 ·°C))	0.48	SC_z	0.54	θ_Z	39.9°
$U_{win,z}$ (W/ (m^2 ·°C))	2.9	$\tau_{win,z}$	1.1	$\underline{T}_z$ (°C)	23
$U_{fl,z}$ (W/ (m^2 ·°C))	0.51	Side 1 (m)	20	$\overline{T}_z$ (°C)	26
$F_{wall,z}$ (m^2)	600	Side 2 (m)	40	$\underline{P}_{HVAC,z}$ (kW)	0
$F_{win,z}$ (m^2)	450	Height (m)	5	$\overline{P}_{HVAC,z}$ (kW)	46

PV parameters	
n_{PV}	0.97
P_{panel} (W)	375
$P_{PV,N}$ (kW)	219
Panel side 1	1.7
Panel side 2	1.016

WG parameters			
NO WGs	5	V_{cut-in} (m/s)	3
$P_{WG,N}$ (kW)	50	$V_{cut-out}$ (m/s)	25
V_N (m/s)	11	n_{WG}	0.85

Electric car parking parameters			
Total cars	100	Parking lots	40

Battery parameters					
C_{ESS} (kWh)	900	$\underline{SOC}_{ESS}$ (kWh)	90	n_{aut}	0.75
$\overline{P}_{g,ESS}$ (kW)	150	$\overline{SOC}_{ESS}$ (kWh)	810	$\underline{T}_{aut}$	13:00
$\underline{P}_{g,ESS}$ (kW)	-150	n_{dch}	0.9	$\overline{T}_{aut}$	15:00
$SOC_{ESS}(0)$ (kWh)	270	n_{ch}	0.9		

Electric cars' parameters				
	Car type 1	Car type 2	Car type 3	Car type 4
C_i (kWh)	32.3	16.7	32.3	47.5
$\overline{P}_i$ (kW)	7.2	4.6	7.2	7.5
SOC_{tg} (kWh)	27.4	14.2	27.4	40.4
$\overline{SOC}_i$ (kWh)	29.07	15.03	29.07	42.75
$\underline{SOC}_i$ (kWh)	3.23	1.67	3.23	4.75

Non-Critical electrical loads' parameters	
n_{nCr}	0.25
$\underline{T}_{sh}$	08:00
$\overline{T}_{sh}$	19:00
$\underline{n}_{sh}$	0.4
$\overline{n}_{sh}$	1.6

Thermal loads ($P_{j_{th}}$) per person (W)			
Human body	100	Display	60
PC	70	Charger	20
Printer	40	Lighting	30

Electrical loads ($P_{j_{el}}$) per person (W)			
Scanner	75	Display	100
PC	500	Charger	100
Printer	110	Lighting	120

In Figure 5.2, the electricity price forecast (EP) that has been used in scenario I, scenario II and scenario III is shown. As presented, the electricity price peaks it's value during 12:00PM-14:00PM. In this case, it is expected that the EMS will prevent the microgrid from consuming power from the utility grid. Instead, it will sell the energy storage units' (building ESS and electric vehicle parking battery) energy during this time period.

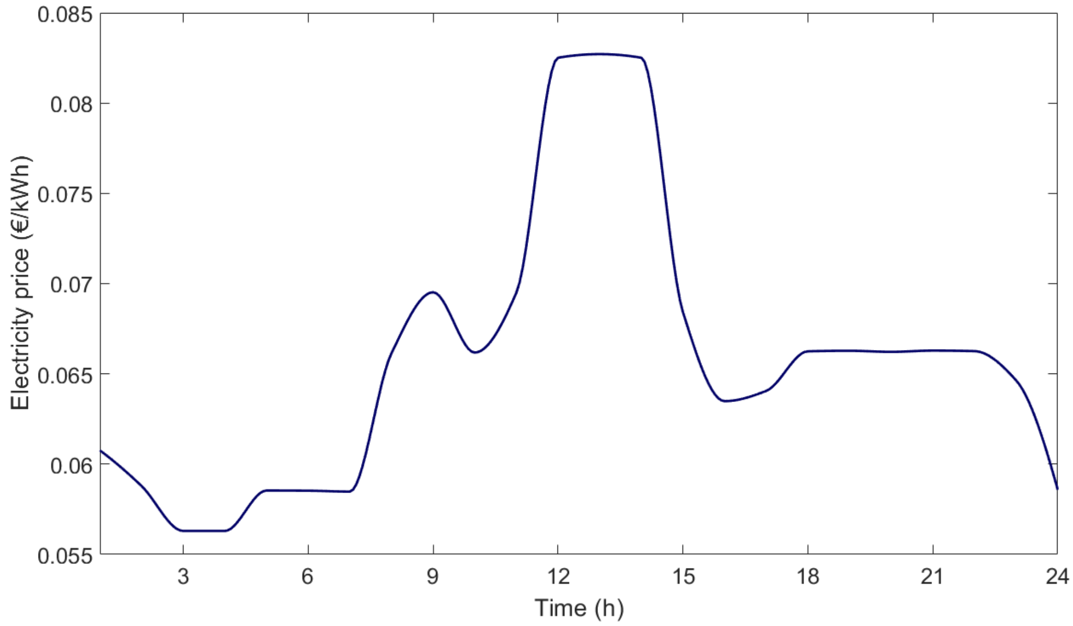

Figure 5.2 Electricity price during the day

The ambient temperature forecast $\hat{T}_{amb}$ is presented in Figure 5.3. It has been used in PMU, to optimize the HVAC electrical power consumption.

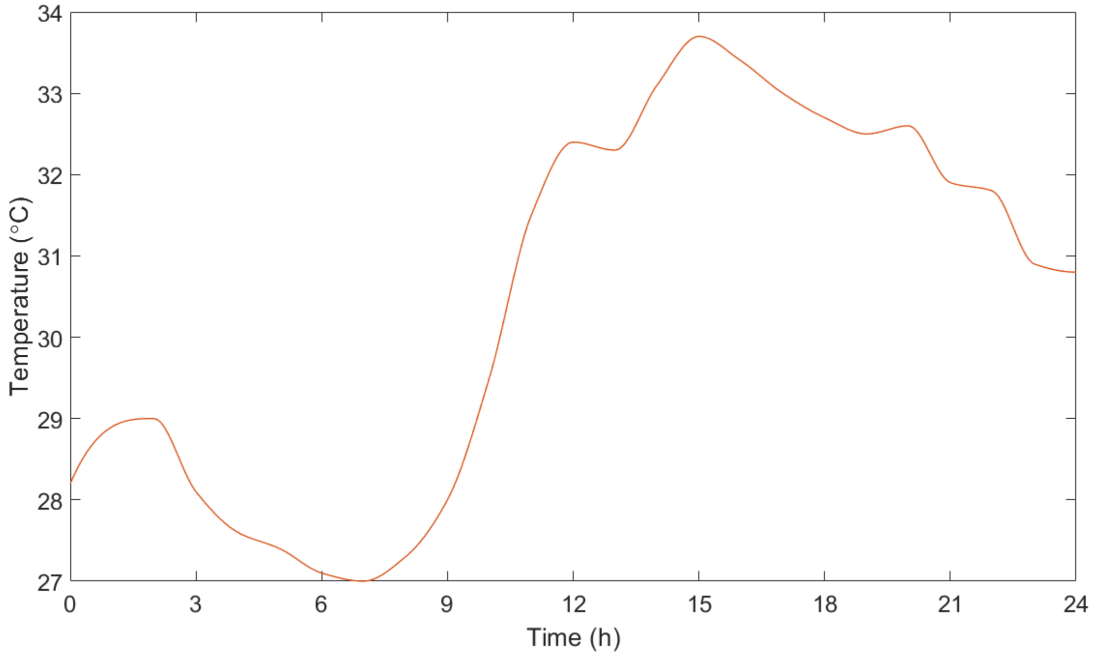

Figure 5.3 Ambient temperature

The forecasted number of people, having activity in each thermal zone, ($\widehat{N}_{P,z}$) is shown in Figure 5.4. It can be observed that this forecast varies for each thermal zone. The prediction of the number of people in a thermal zone has been used in THLPC and CELPC (and consequently in nCELPC), to create the thermal and electrical load profiles of each building.

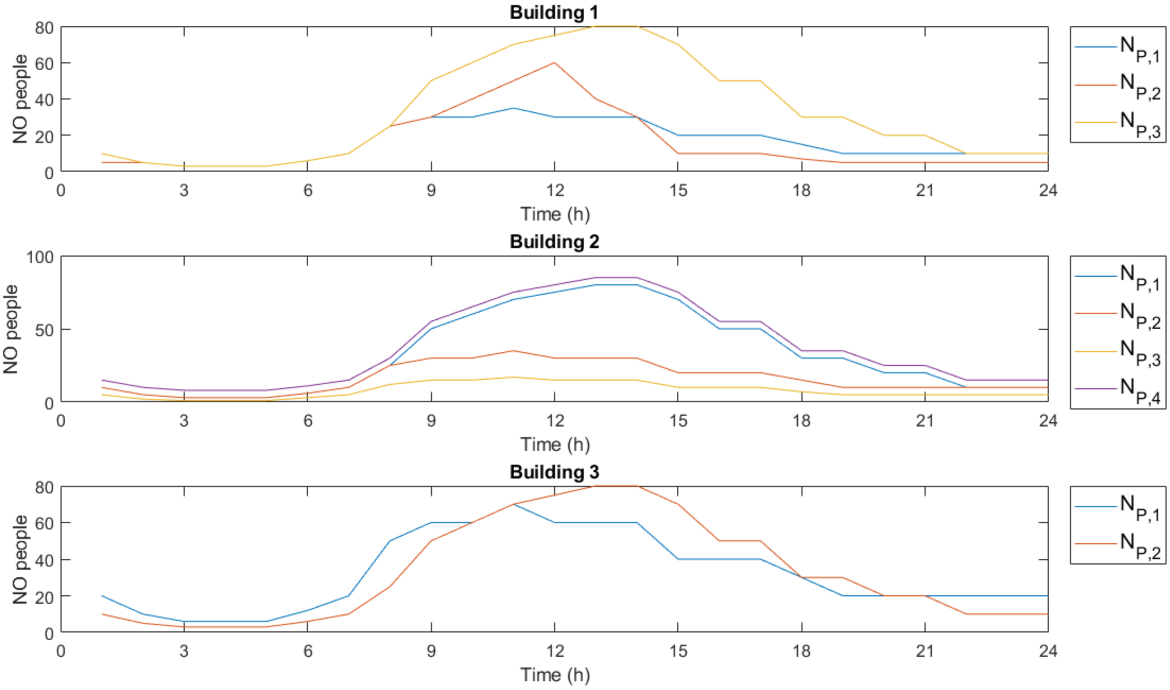

Figure 5.4 Number of people in every thermal zone of every building

The beam, diffuse and total radiation ($\hat{I}_b$, $\hat{I}_d$ and $\hat{I}$) forecasts are shown in Figure 5.5. Figure 5.6 shows the forecasted wind velocity $\hat{V}$. PVGPC and WPPC, that were described in section 4.2, create power generation profiles from photovoltaics and wind generators activity, using these forecasts. The photovoltaic unit was assumed to having 85% coverage of each building's roof.

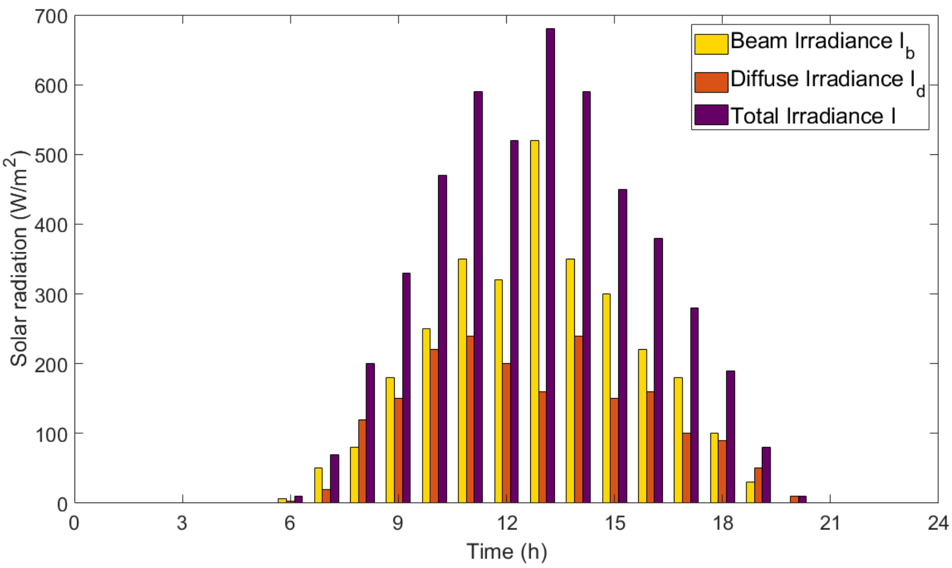

Figure 5.5 Solar radiation

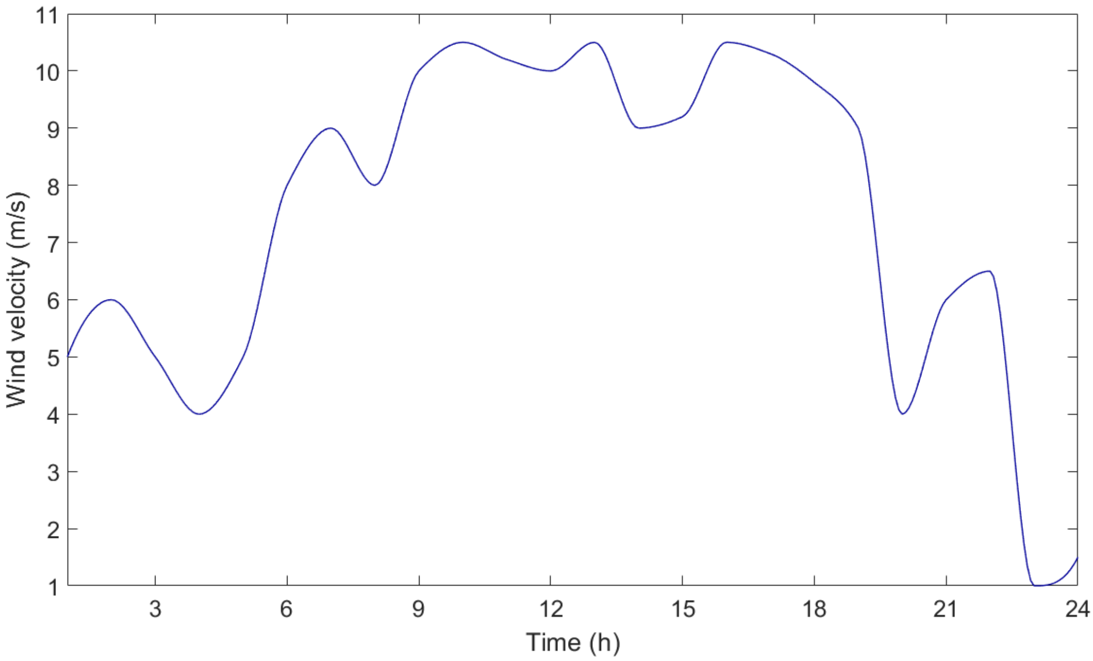

Figure 5.6 Wind velocity

In Figure 5.7, the forecast of the number of the plugged-in electric vehicles (PEVs) of the electric vehicle parking lot of the microgrid is shown. The probability density functions used for the initial state of charge ($\mathrm{SoC_i}(\mathrm{t_{0,i}})$), the arrival time of a PEV ($\mathrm{t_{0,i}}$) and the staying time of a PEV ($|t_{f,i} - t_{0,i}|$) are shown in Figure 5.8, Figure 5.9 and Figure 5.10 respectively. These probability density functions have been used in EVPLA, in order to estimate the equivalent battery model of the electric vehicle parking lot.

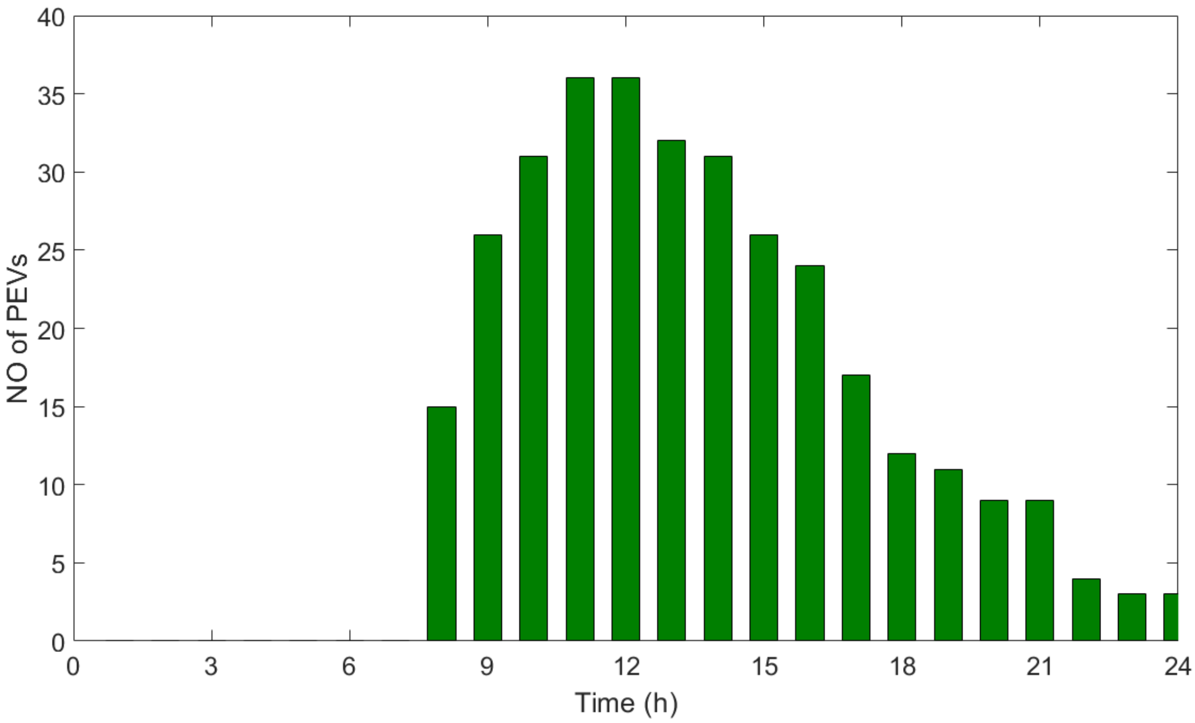

Figure 5.7 Number of connected EVs to the microgrid

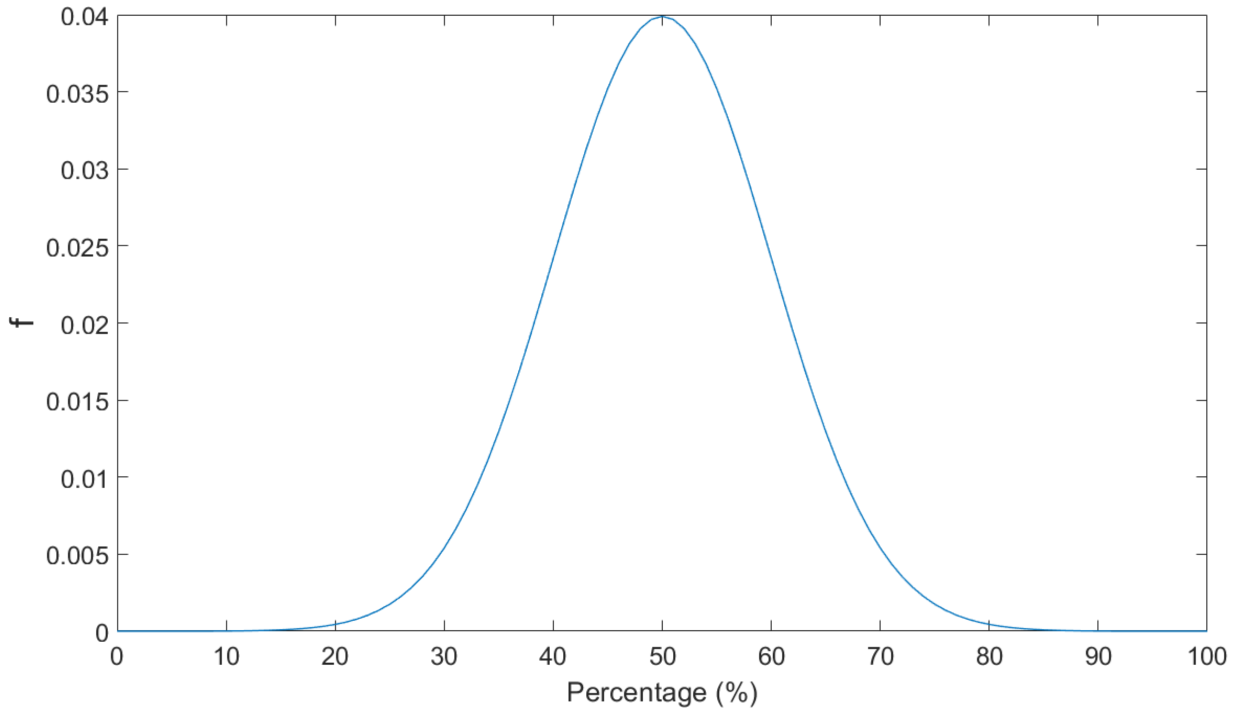

Figure 5.8 Initial state of charge, $SoC_i(t_{0,i})$, probability density function

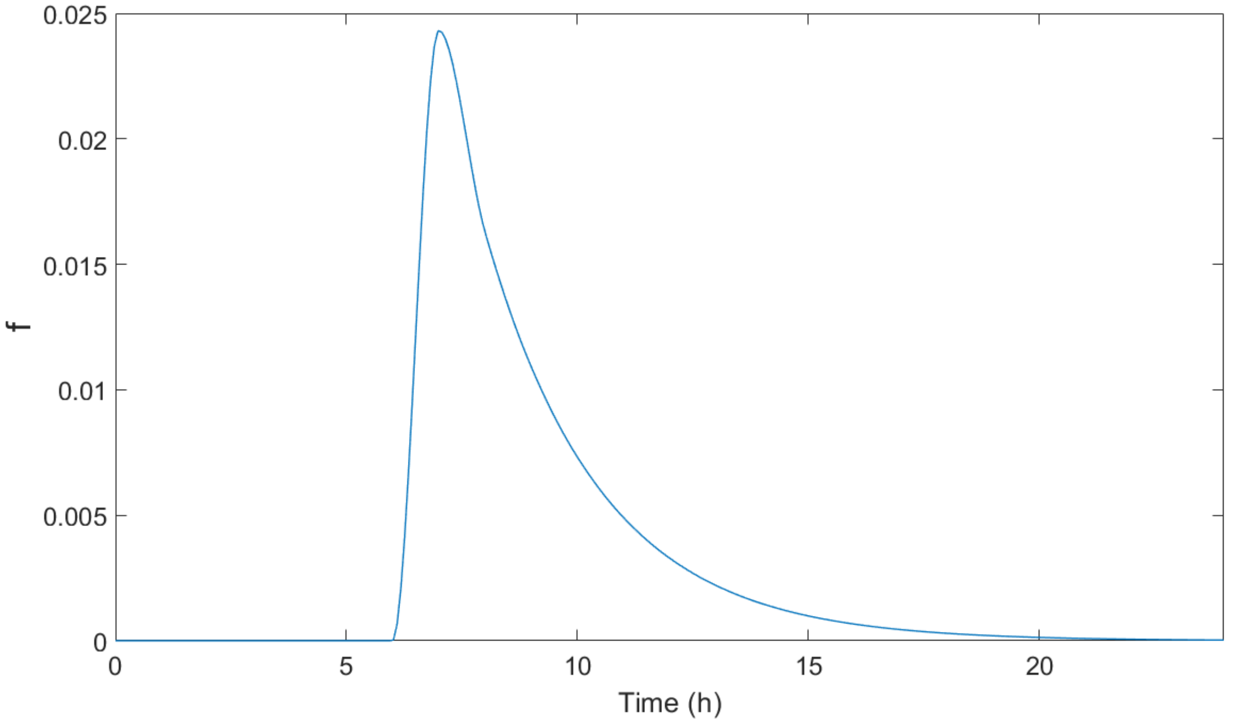

Figure 5.9 Arrival time, $t_{0,i}$, probability density function

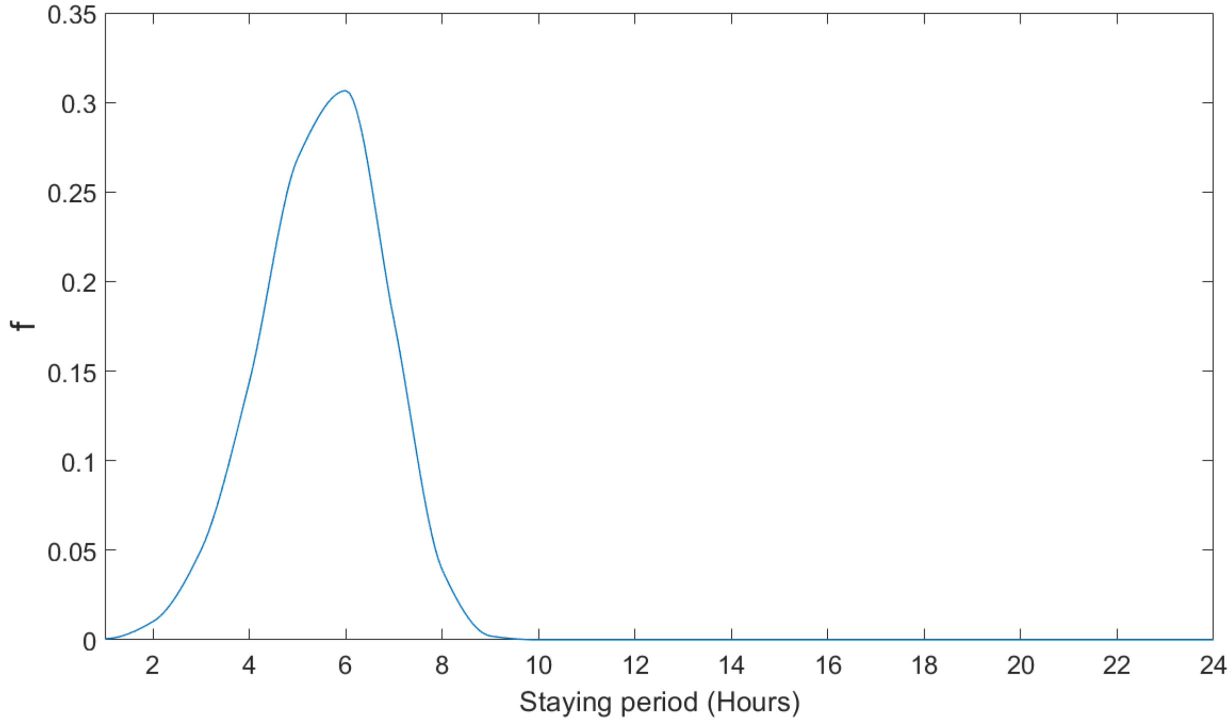

Figure 5.10 Parking period, $t_{f,i} - t_{0,i}$, probability density function

As shown in Figure 4.4, the first level of optimization follows the step of profile creators (THLPC, CELPC, nCELPC, PVGPC, WPPC, EVPLA). In this step, the PMU optimizes the HVAC system operation and the non-critical electrical load consumption of every building's thermal zone. The last step shown in Figure 4.4, is the second level of optimization that estimates the optimal power exchange between the microgrid's ESUs and the utility grid.

A set of different scenarios are presented next in order to examine the proper functioning of the EMS. The first, scenario minimizes the operating cost of the microgrid that was described above. In the second scenario, it is assumed that a power outage will occur during 13:00PM-15:00PM. While, the third scenario presents the typical operation of a microgrid (business as usual), without any step of the optimization process applied. In the fourth scenario, the operation of the microgrid for scenario I, scenario II and scenario III is presented for a time period of a week.

5.2 Scenarios for one day

5.2.1 Scenario I

This scenario optimizes the operation of the microgrid, based on the data presented in the case study. This scenario aims to minimize the microgrid's overall operating cost.

The HVAC electrical loads ($P_{HVAC,z}$) and the internal temperatures (T_z) of each thermal zone for building 1, building 2 and building 3 are shown in Figures 5.11, 5.12 and 5.13, respectively. The HVAC power consumption shown in these figures, results from the first level of optimization.

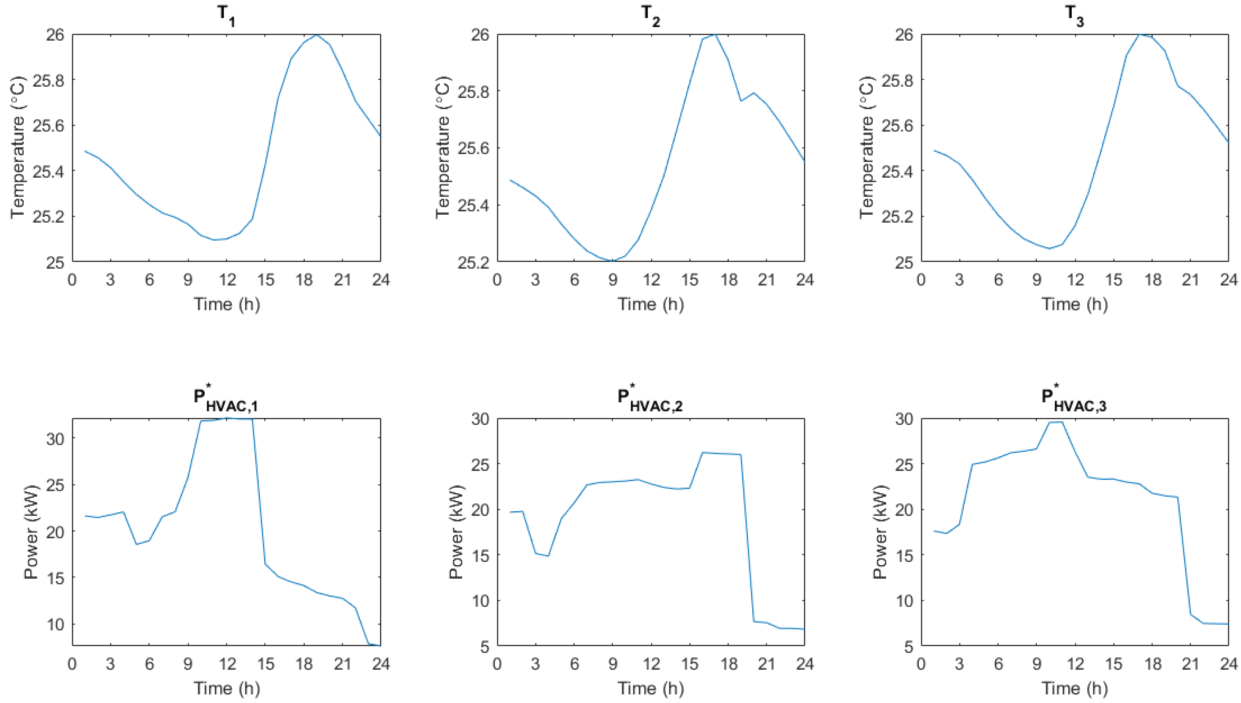

Figure 5.11 HVAC system of building 1

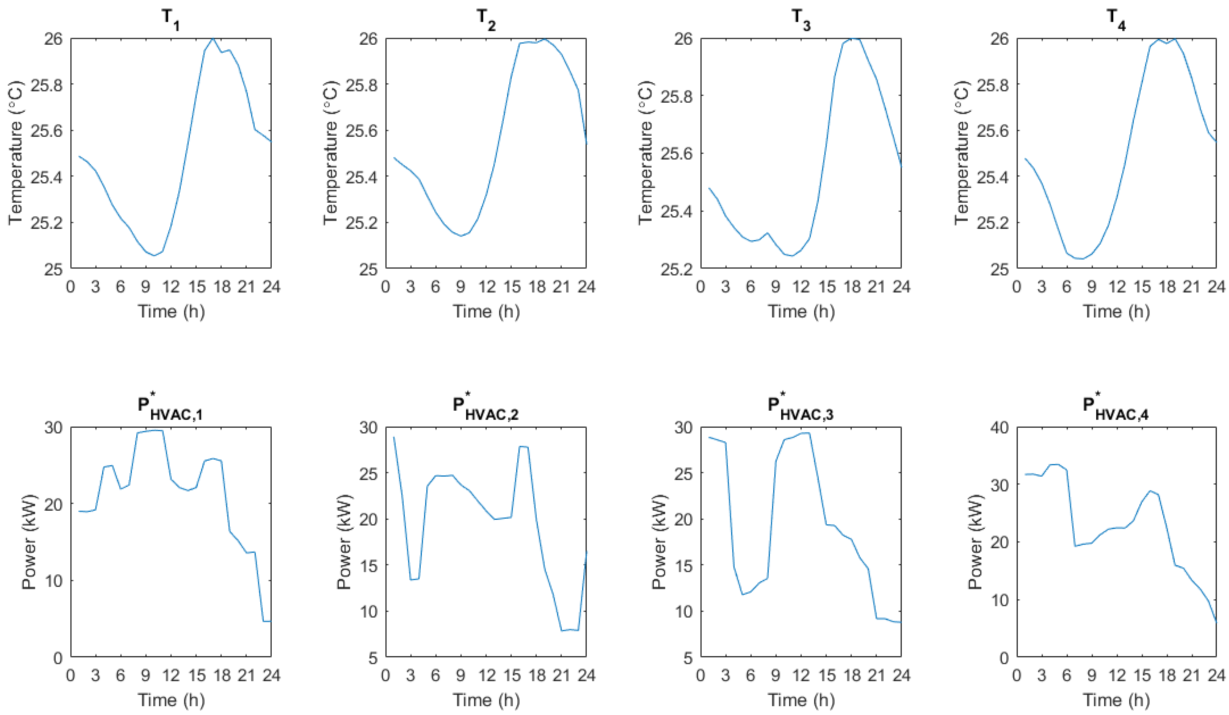

Figure 5.12 HVAC system of building 2

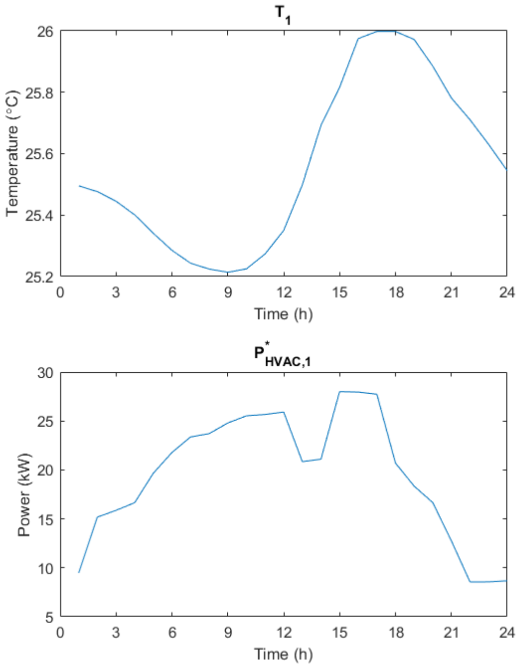

Figure 5.13 HVAC system of building 3

It appears that the EMS uses the HVAC system to lower the temperature value in the thermal zones, at time periods that the electricity price is low. While, allowing the temperature value to rise, in time periods that the electricity price is high. Nevertheless, the temperature value in every zone remains in between the constraint values.

Furthermore, the electrical critical loads (P_{el}) and the electrical non-critical loads (P_{nCr}) of the buildings, that have arisen after the first level of optimization, are shown in Figure 5.14.

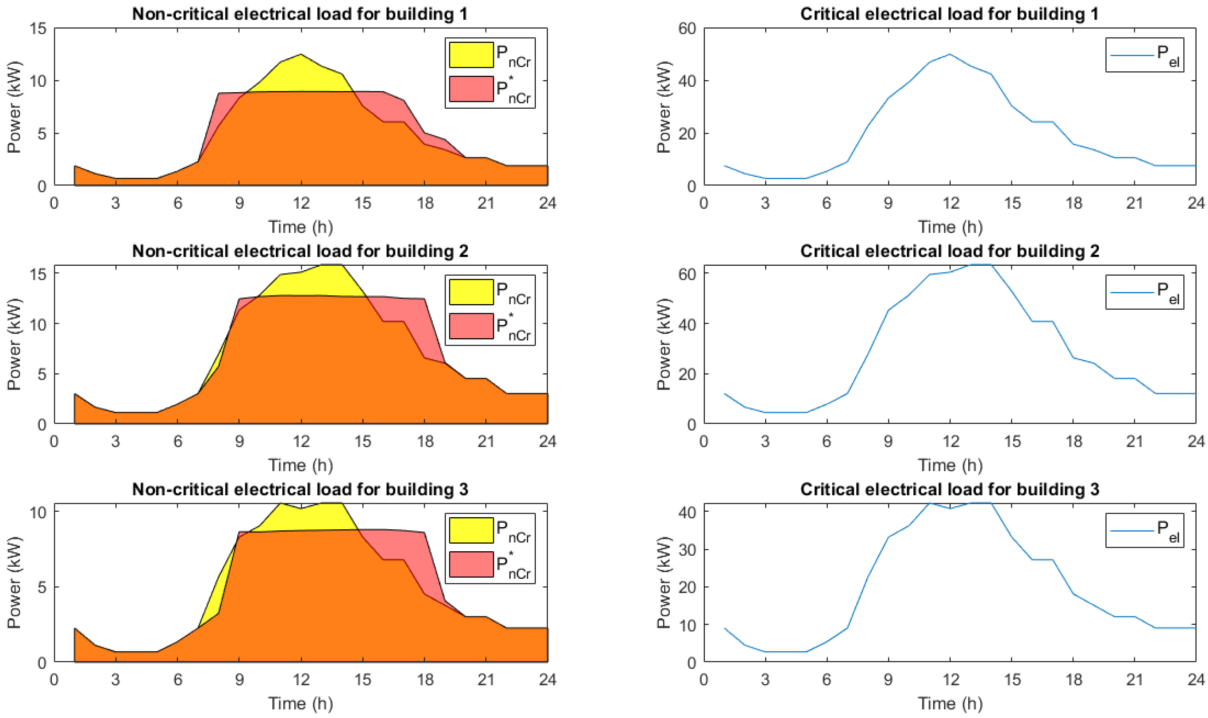

Figure 5.14 Buildings' critical and non-Critical electrical loads

It is observed that the non-critical electrical loads have been optimally shifted, to time periods where the electricity price is lower. The critical electrical loads shown in the same Figure are those resulting from CELPC. In addition, the photovoltaics' (P_{PV}) and wind generators' (P_{WG}) power generation profiles are shown in Figure 5.15.

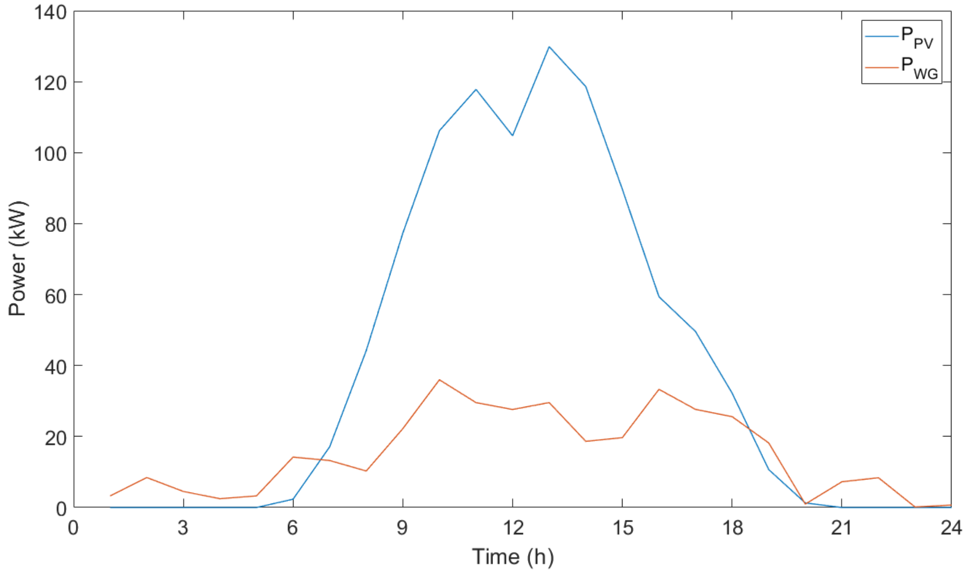

Figure 5.15 Power generation profiles of photovoltaics and wind generators

To conclude this scenario, the state of charge and the power consumption, of the building ESS and the electric vehicle parking lot battery, resulting from the second level of optimization are shown in Figure 5.16. while Figure 5.17 shows the results of the two energy storage units as one equivalent battery.

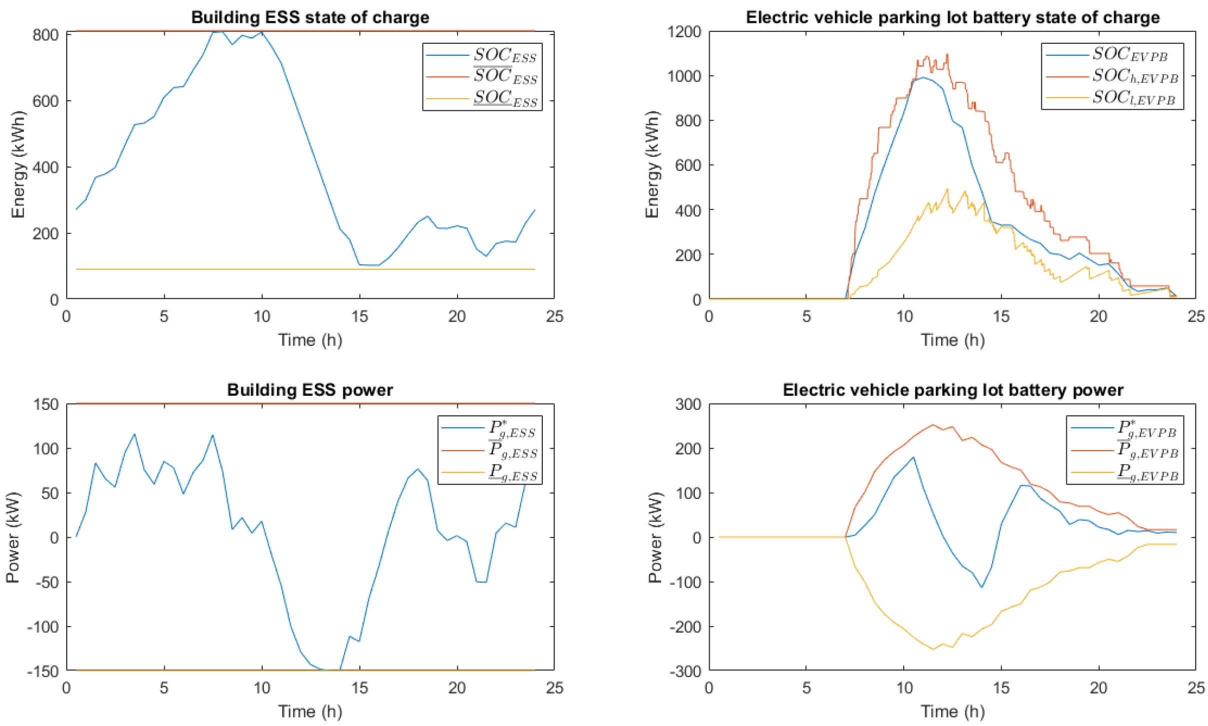

Figure 5.16 Optimal use of microgrid's ESUs

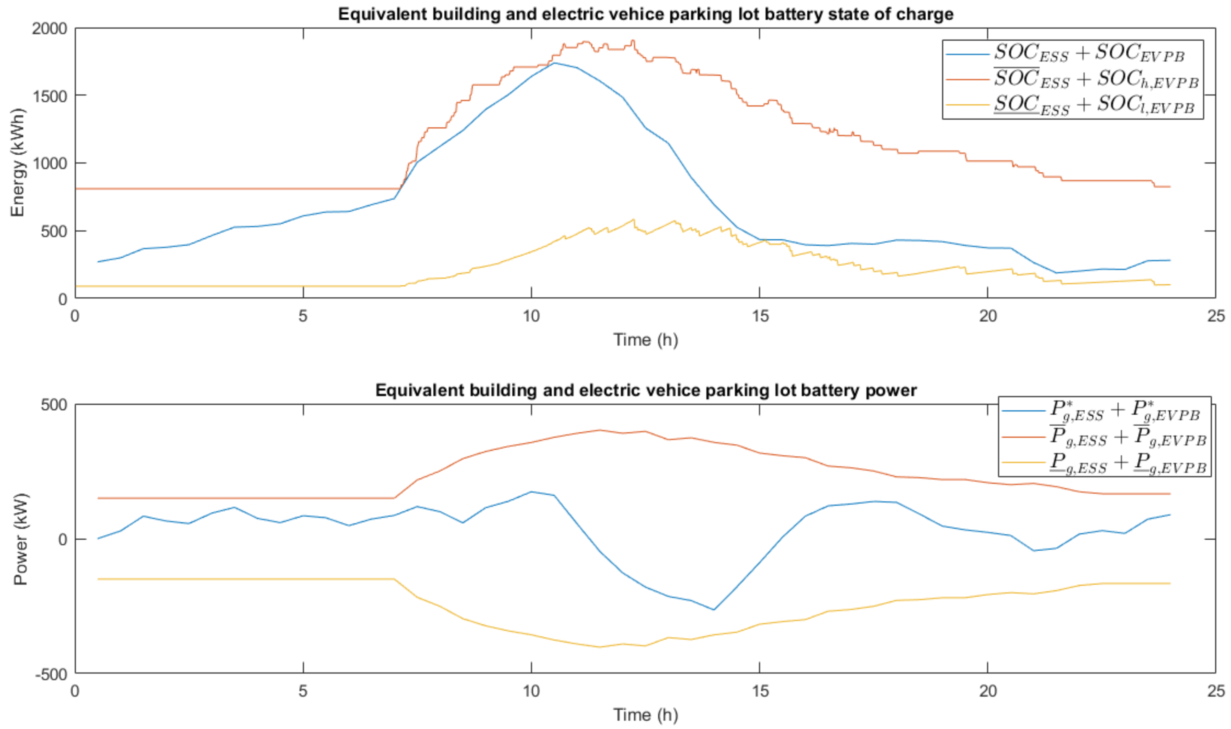

Figure 5.17 ESUs as an equivalent battery

It is observed that both energy storage units draw power during the 01:00AM-11:00AM time period, when the price of electricity is low. Subsequently, the two ESUs sell the stored energy, when the electricity price is increased to reduce the cost of network operation.

5.2.2 Scenario II

The second scenario considers the same date of 15th of July 2019. The same forecasts of electricity price, ambient temperature, sun radiation, wind velocity, number of people and number of EVs are considered as well. The only difference from the previous scenario, is that it is assumed a power supply interruption from the utility grid during 13:00PM-15:00PM time period. So, it is expected that the energy storage units will charge as much as possible, to cover the 75% of the total microgrid's energy needs.

The 75% of the total electrical load consumption in the microgrid is presented in Figure 5.18, while in Figure 5.19 are shown the state of charge and the power consumption of the building ESS and the electric vehicle parking lot battery, resulting from the second level of optimization. In Figure 5.20 are shown the two energy storage units as one equivalent battery.

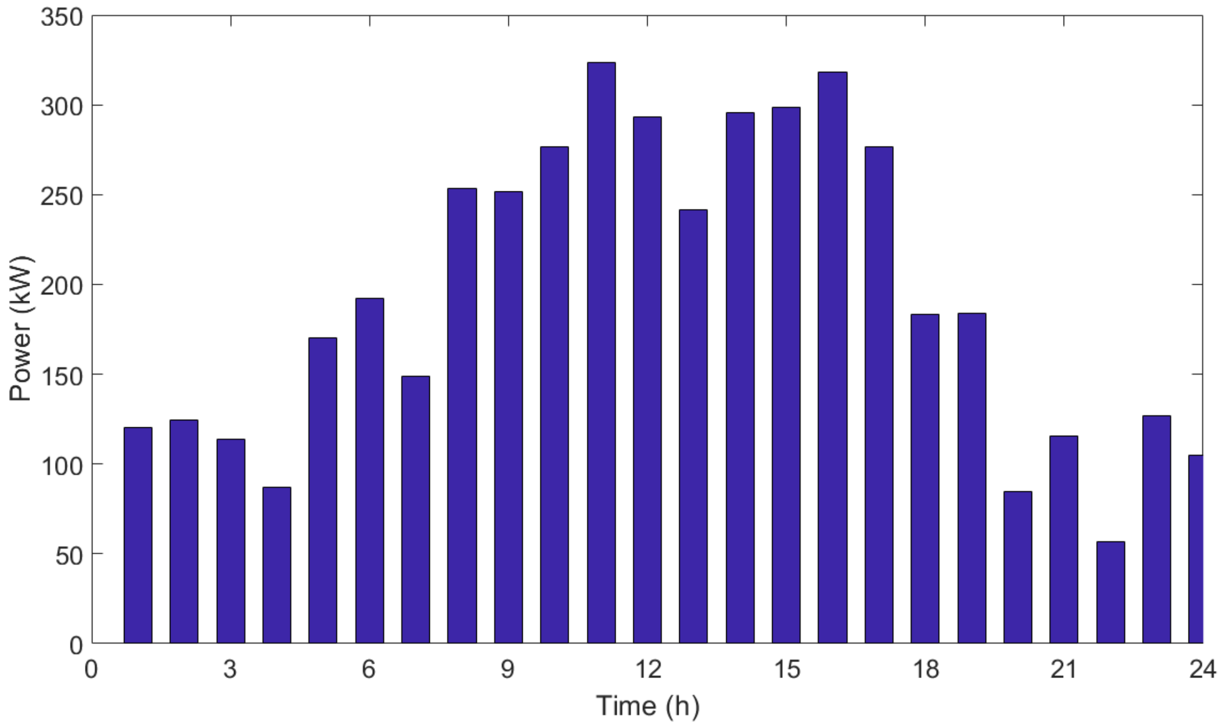

Figure 5.18 75% of the total electrical loads of the microgrid

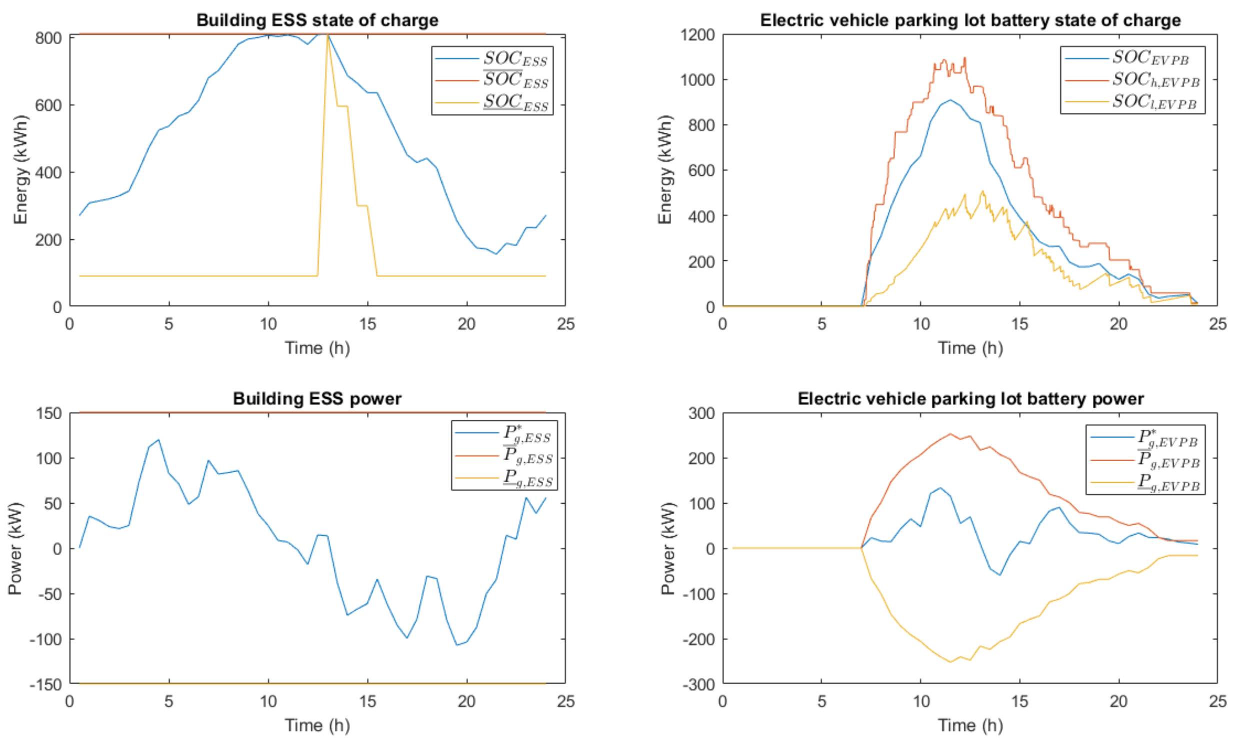

Figure 5.19 Optimal use of microgrid's ESUs for scenario II

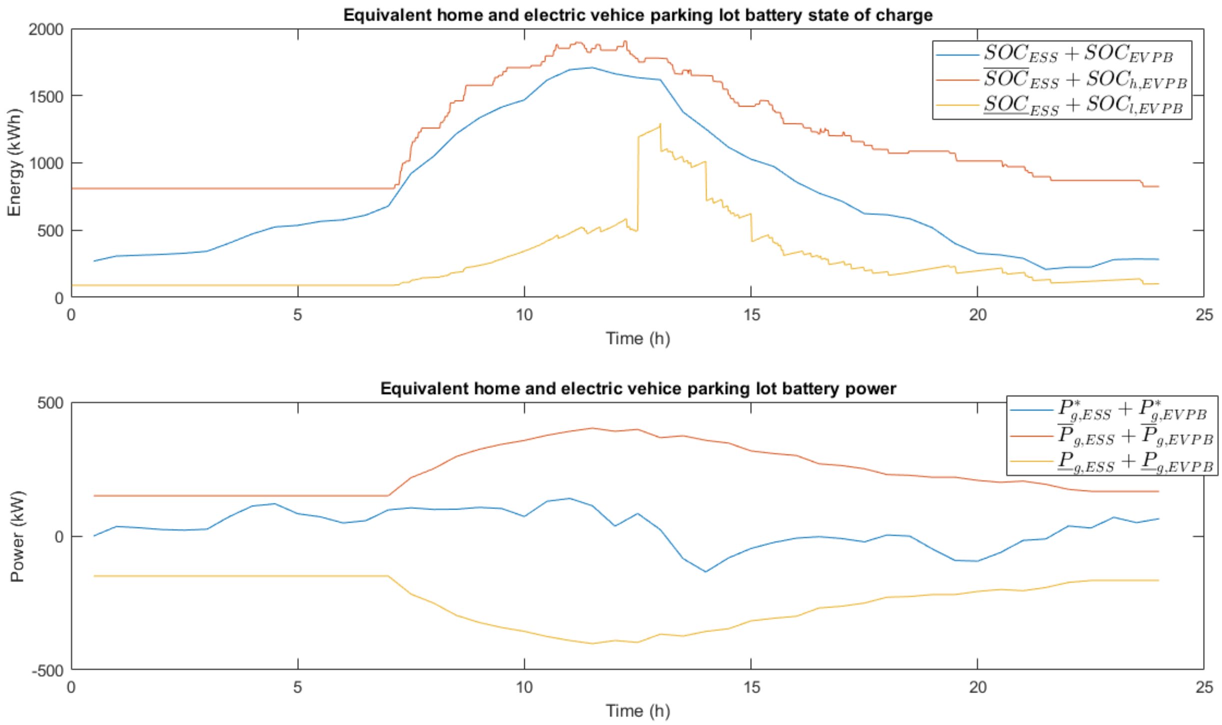

Figure 5.20 ESUs as an equivalent battery for scenario II

Therefore, it can be noted that the EMS prioritizes to satisfy the microgrid's energy needs and then tries to minimize the microgrid's operation cost for this particular scenario, by selling the remaining stored energy at a higher price than it was purchased. However, an increase in the total microgrid operation cost is expected.

5.2.3 Scenario III

In the third scenario, is performed the operation of the described microgrid without optimizing its operation, or business as usual (BAU). This scenario performs any level of optimization for the HVAC or non-critical electrical loads, makes use of no building ESS and the electric vehicles that are connected to the electric vehicles parking lot, get charged to their target state of charge. The RES' power generation is the same as the previous scenarios.

The electrical loads consumed by the HVAC system ($P_{HVAC,z}$) and the internal temperatures (T_z) of the thermal zones for building 1, building 2 and building 3 are shown in Figure 5.21, Figure 5.22 and Figure 5.23, respectively. While, the electrical critical loads (P_{el}) and the electrical non-critical loads (P_{nCr}) of the buildings are shown in Figure 5.24. Figure 5.25 displays the electric vehicle parking lot battery's state of charge (SOC_{EVPB}) and power consumption ($P_{g,EVPB}$).

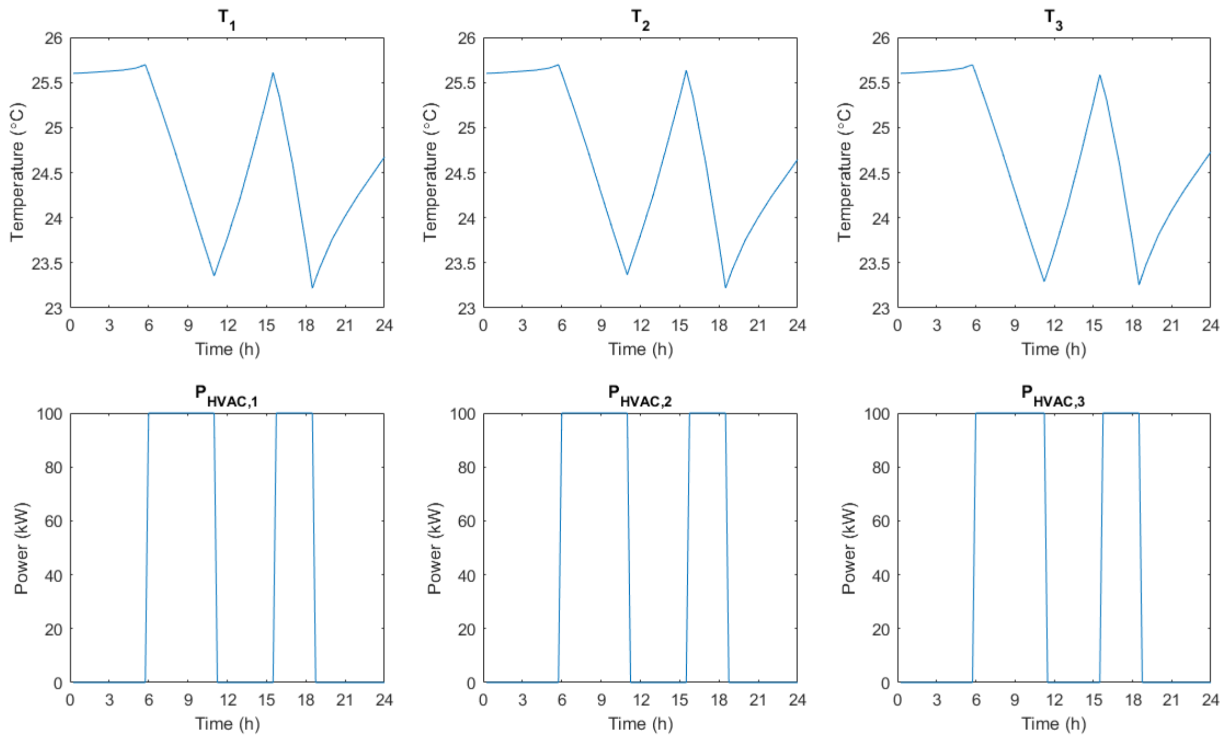

Figure 5.21 HVAC system of building 1

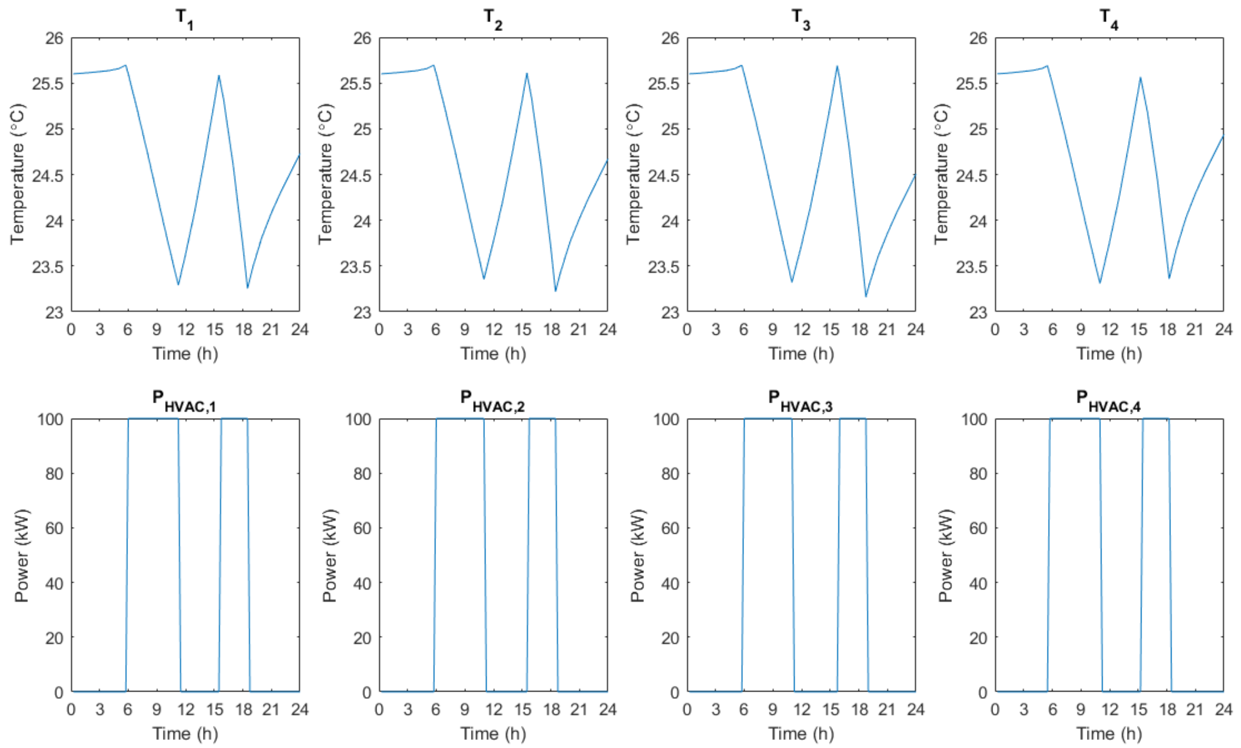

Figure 5.22 HVAC system of building 2

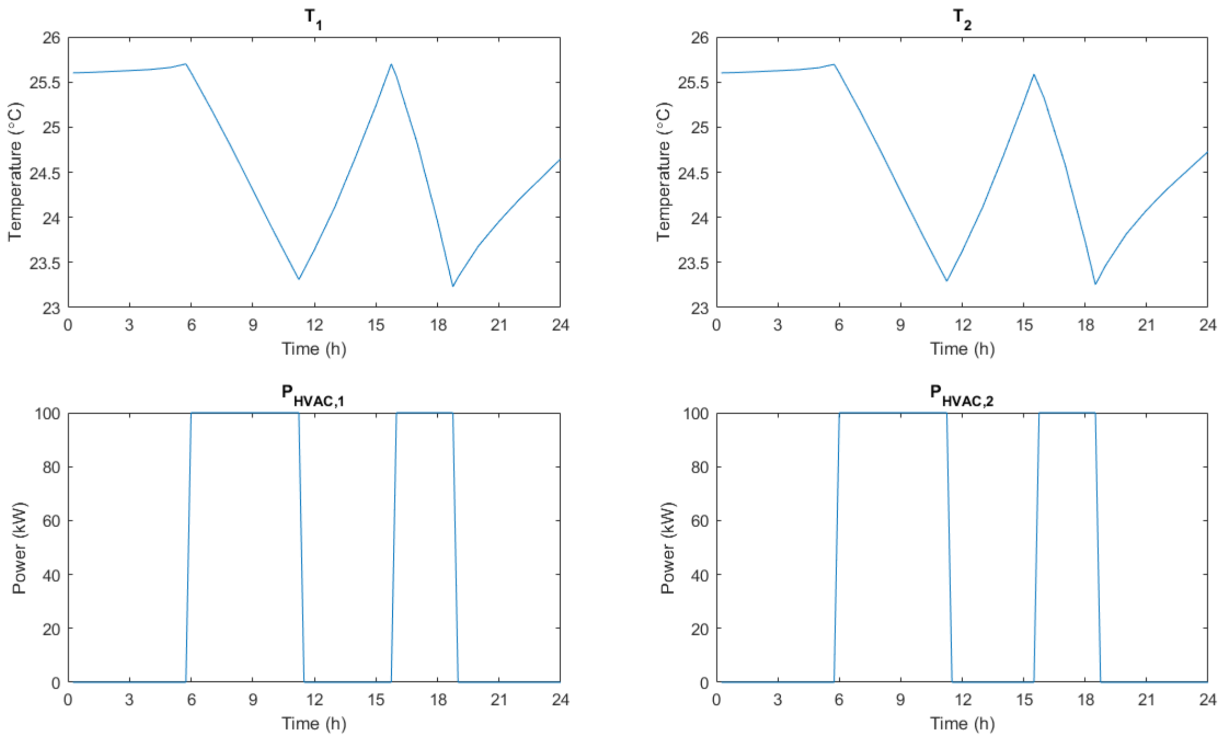

Figure 5.23 HVAC system of building 3

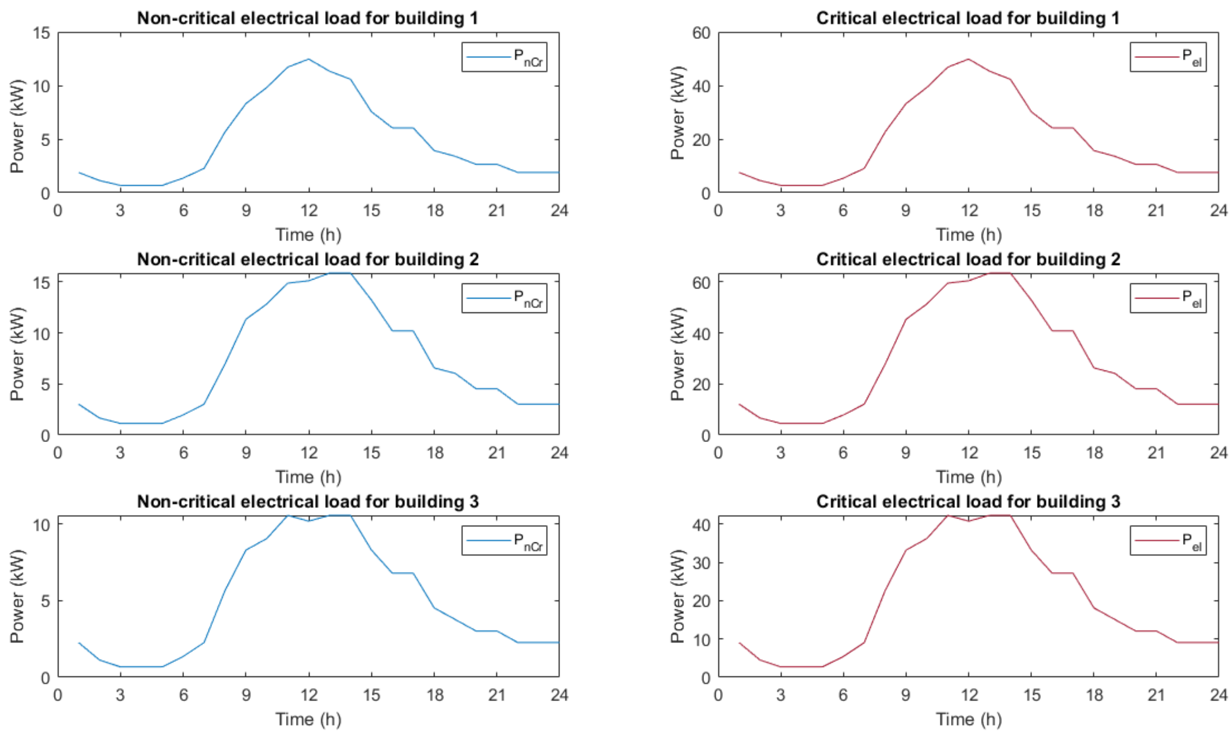

Figure 5.24 Buildings' critical and non-Critical electrical loads

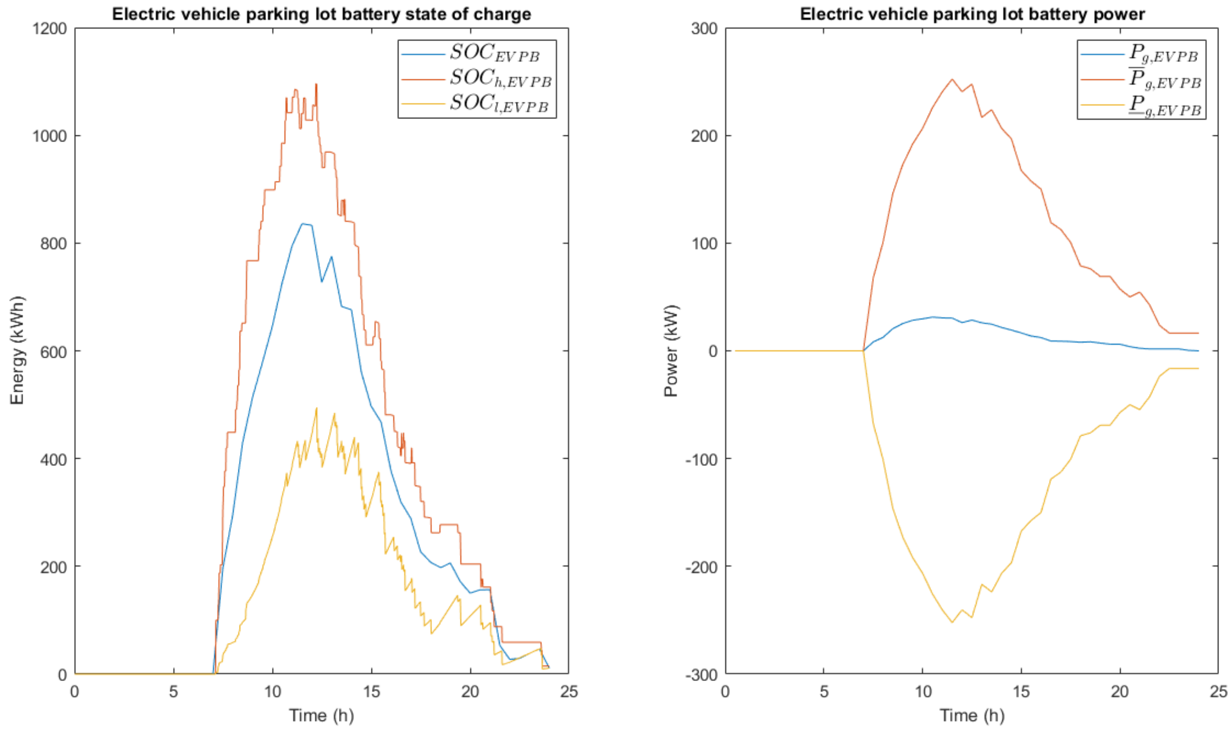

Figure 5.25 Electrical vehicle parking lot battery use in scenario III

In this scenario, the HVAC system works in order to keep every thermal zone's inner temperature, in the expected limits. Nevertheless, an upgrade to a 100 kW system was necessary. This scenario was created to calculate the cost of a common microgrid today and compare it to the proposed EMS solution. So, Table 5.2 demonstrates the total microgrid operation costs for scenario I, scenario II and scenario III.

Table 5.2 Total cost of microgrid's operation for the three different scenarios

Microgrid operating cost (€)	Scenario I	Scenario II	Scenario III
	372.87	383.43	560.26

5.3 Scenario for one week

In this scenario, the microgrid's operation has been simulated, using the three different scenarios created previously, for the time period of one week. The electricity price, ambient temperature, sun radiation and wind velocity forecasts from 4th to 10th of July 2019 in Attica area were used. So, the HVAC system, critical and non-critical electrical loads of the buildings, resulting from the first level of optimization in scenario I are shown in Figure 5.26. While, Figure 5.27 demonstrates the corresponding loads for scenario III.

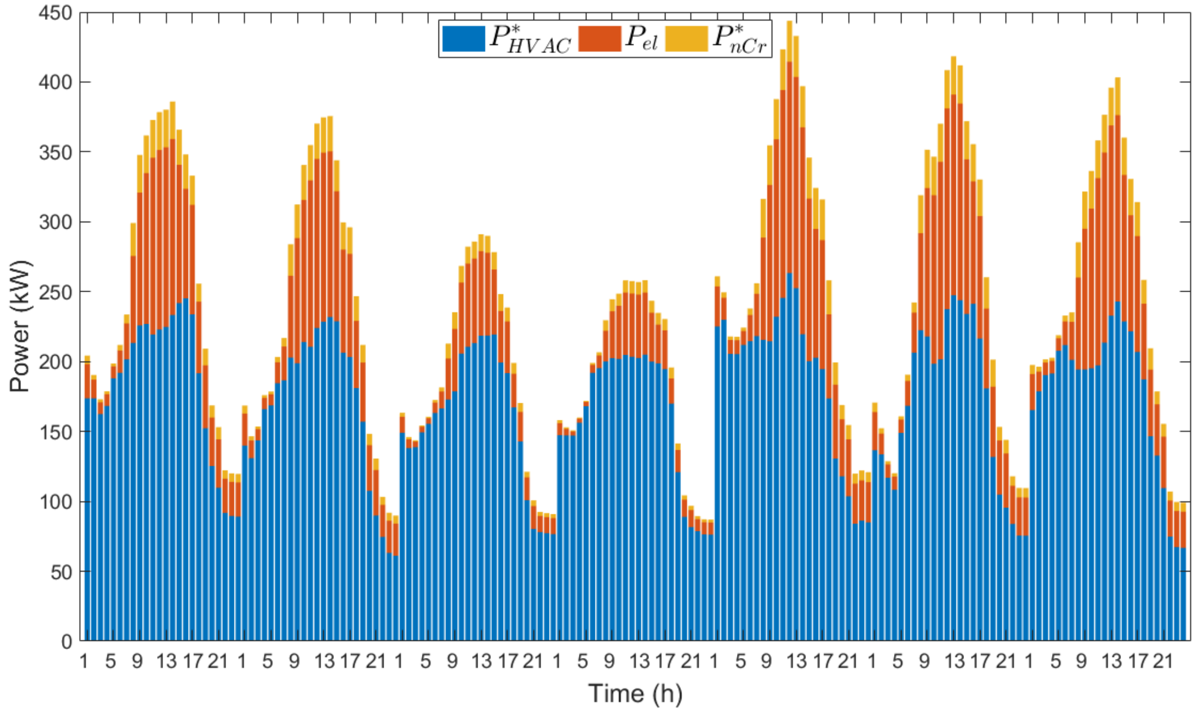

Figure 5.26 Buildings' total loads in scenario I

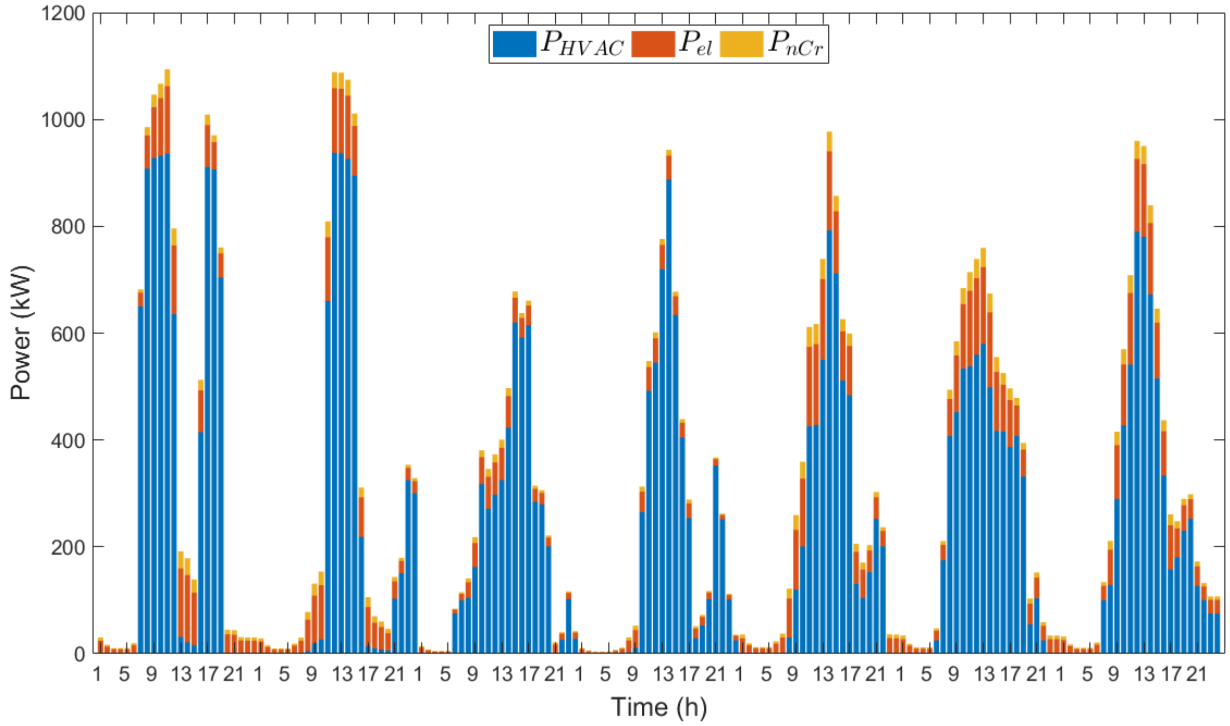

Figure 5.27 Buildings' total loads in scenario III

The non-critical electrical loads before and after the first level of optimization are shown in in Figure 5.28.

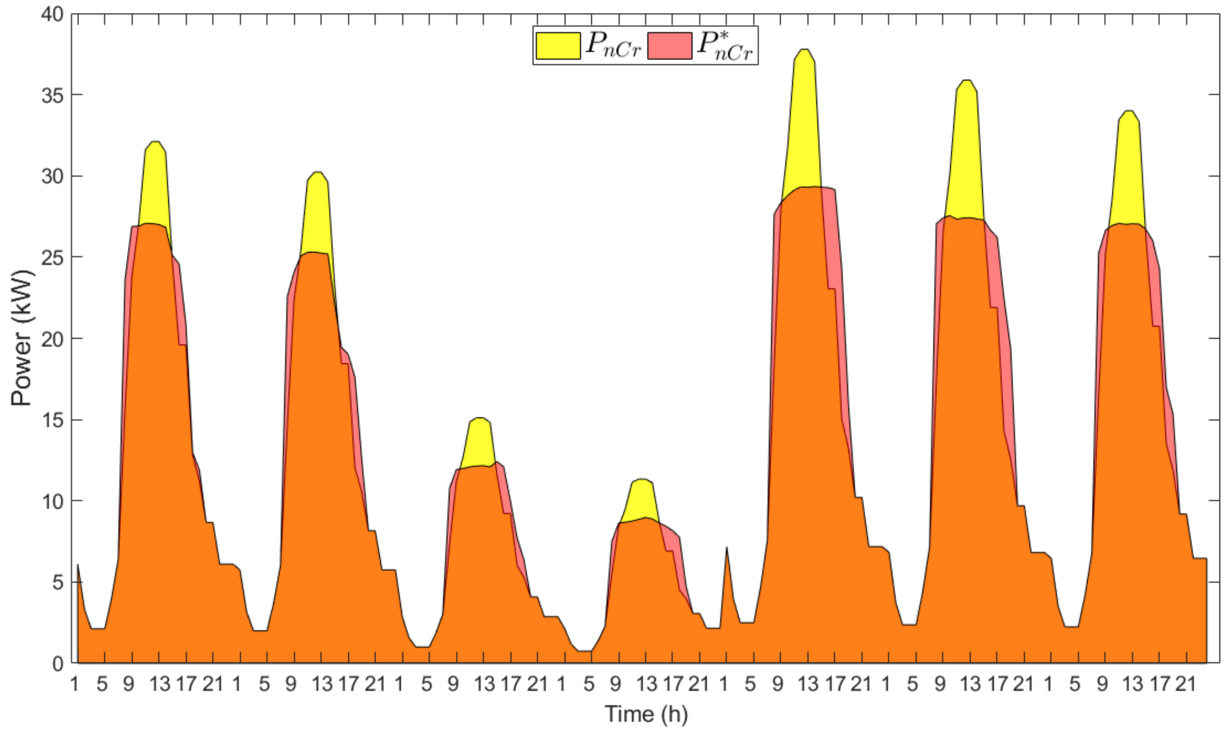

Figure 5.28 Total non-Critical electrical loads before and after the first level of optimization

The internal temperature of all of the buildings' thermal zones for scenario I and scenario III, including the outer temperature, are shown in Figure 5.29 and Figure 5.30, respectively.

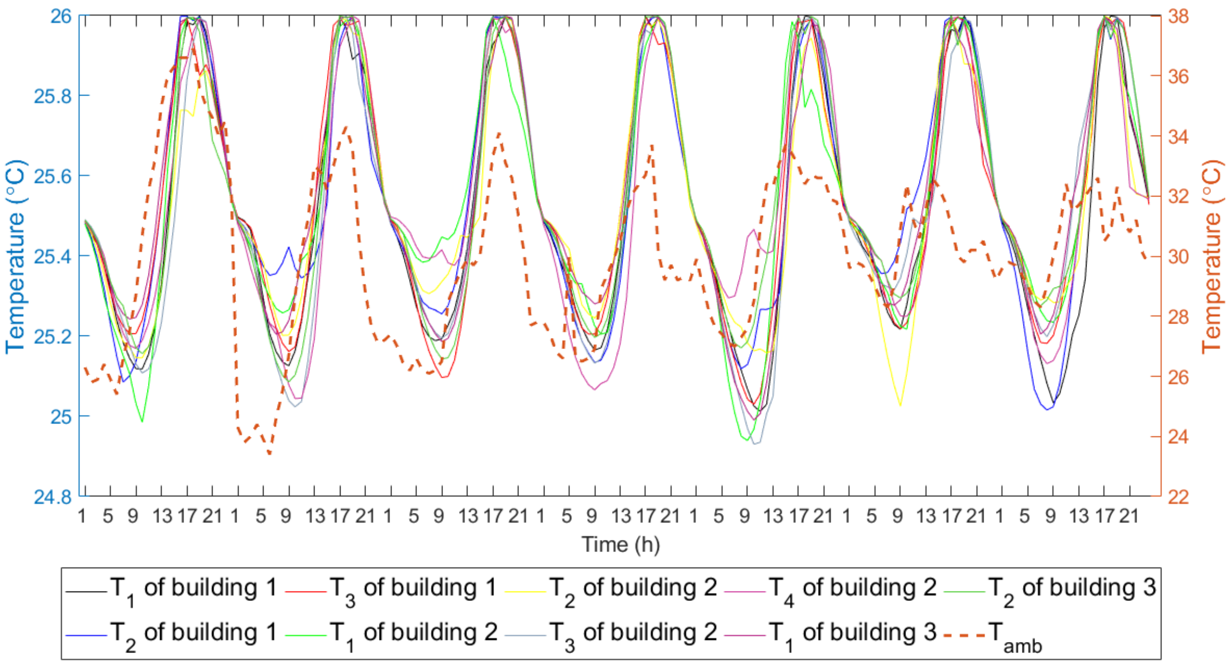

Figure 5.29 Internal temperature of every building's thermal zone for scenario I

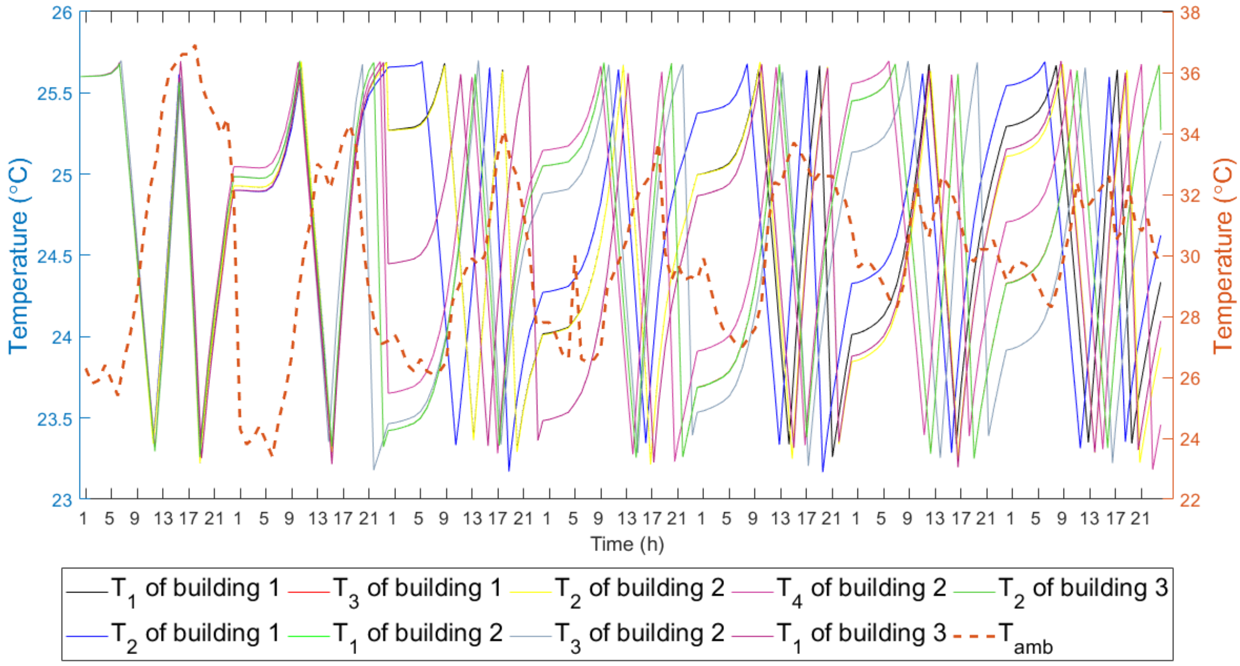

Figure 5.30 Internal temperature of every building zone for scenario III

RES power generation during the week is displayed in Figure 5.31. While the total electrical energy, stored by the microgrid's ESUs (building ESS and electric vehicle parking lot battery) for scenario I, scenario II and scenario III, is shown in Figure 5.32, Figure 2.33 and Figure 2.34 respectively.

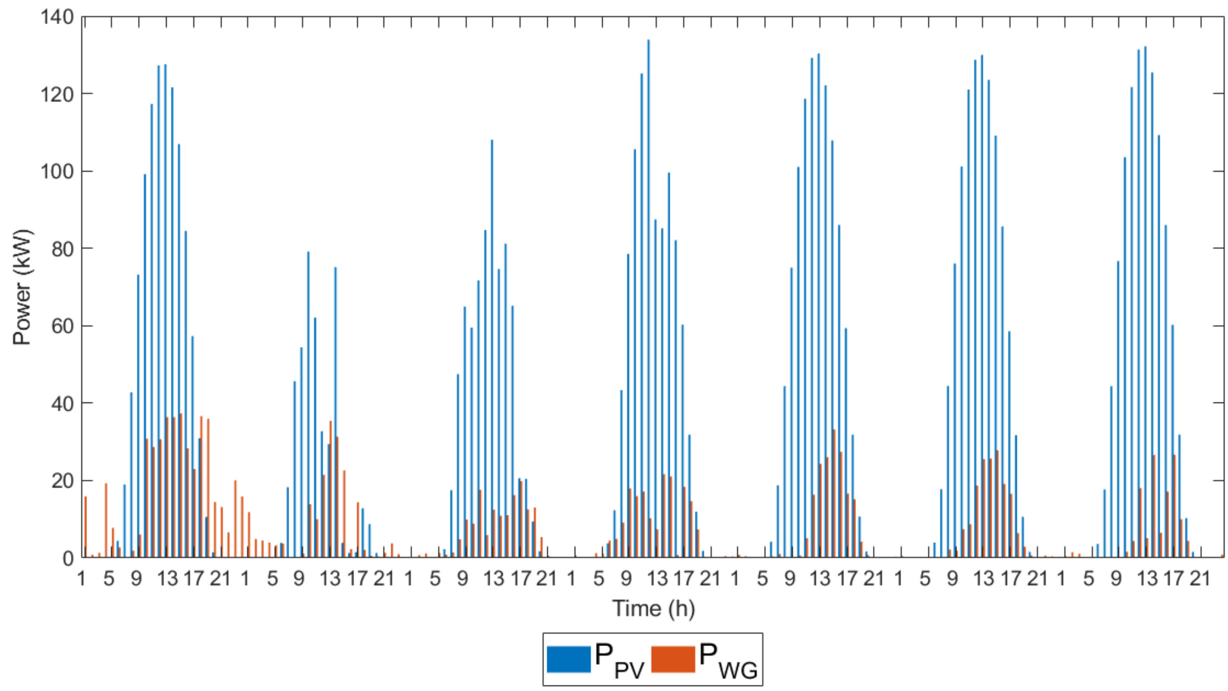

Figure 5.31 RESs power generation

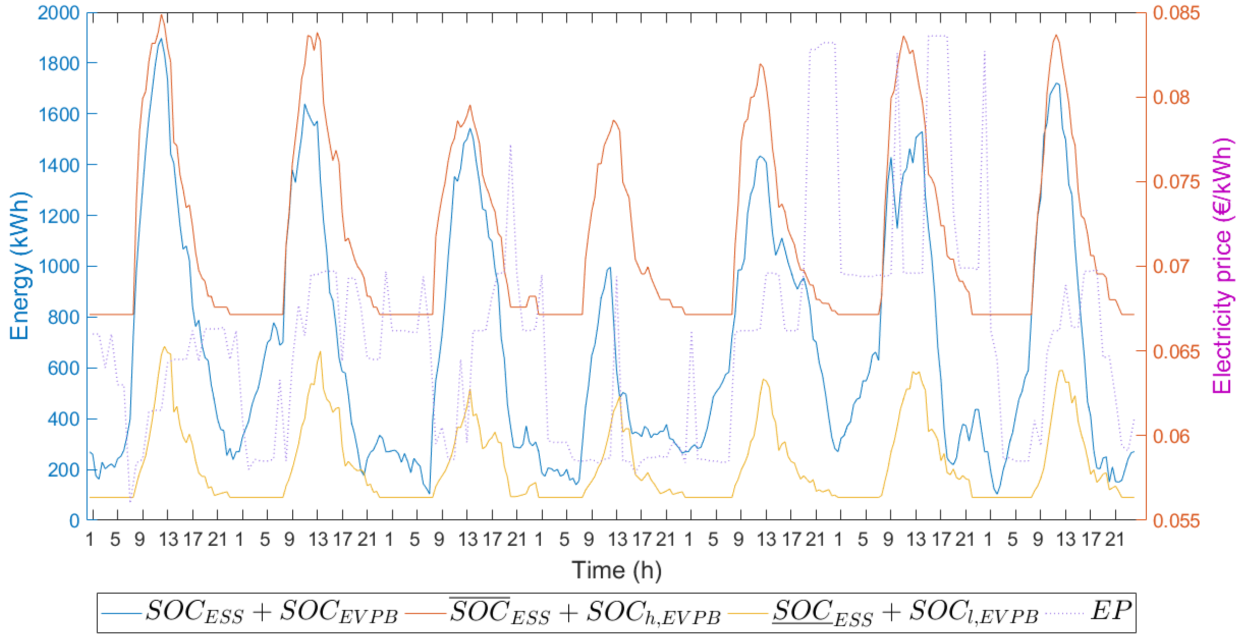

Figure 5.32 ESUs as an equivalent battery of scenario I for a week

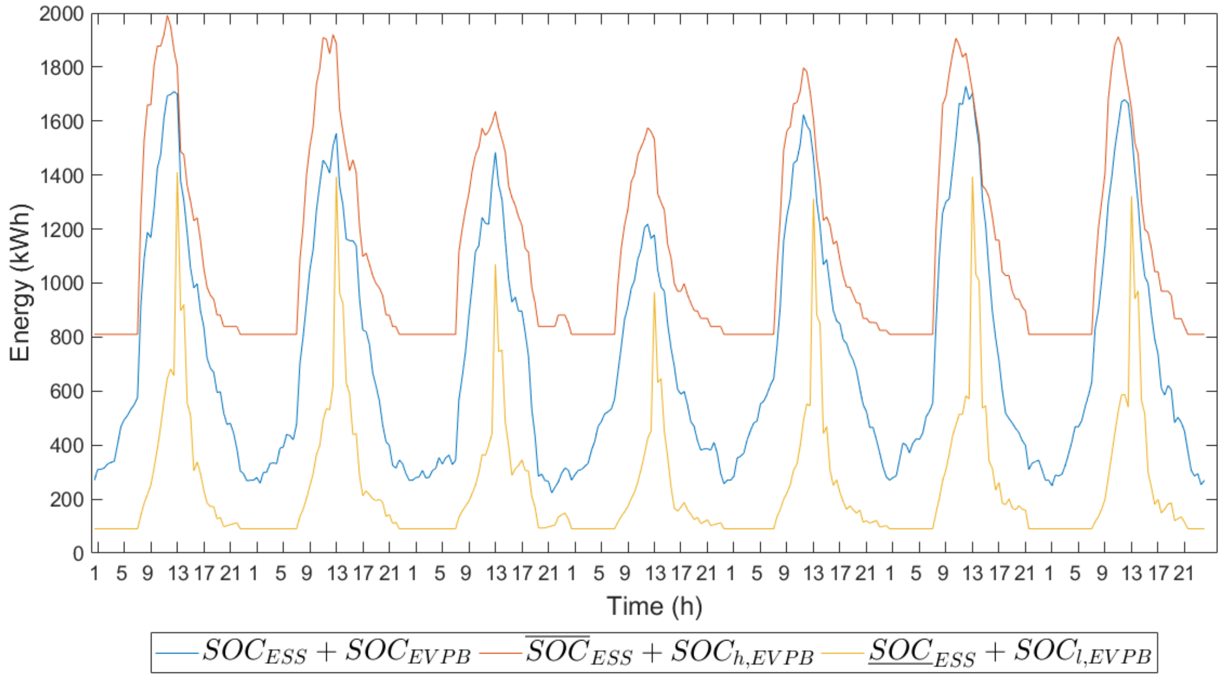

Figure 5.33 ESUs as an equivalent battery of scenario II for a week

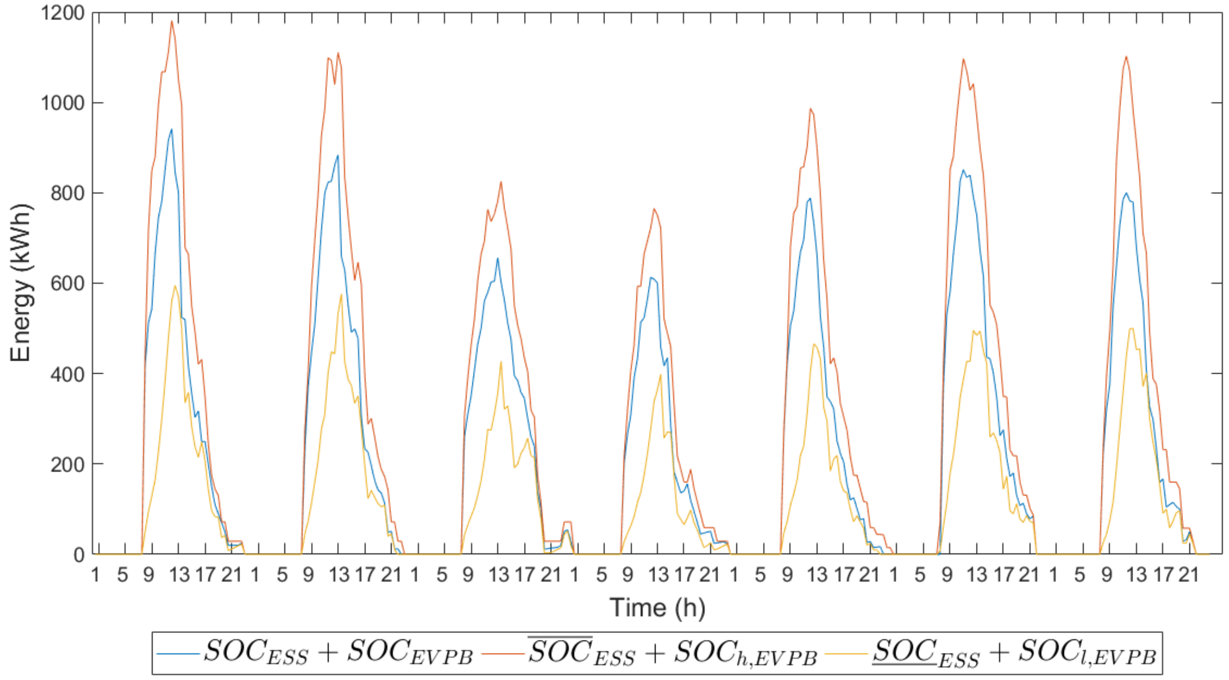

Figure 5.34 ESUs as an equivalent battery of scenario III for a week

As shown in Figure 5.26, the HVAC system, critical and non-Critical electrical loads vary during the week because of the different number of people having activity in the buildings every day. The Non-Critical electrical loads profile, shown in Figure 5.28, has been optimized based on the electricity price of each day. As shown in Figure 5.29, internal temperatures of each thermal zone are kept into the permissible limits that was declared in Table 5.1. Continuing to Figure 5.32, it is recognized the different use of the equivalent microgrid's ESUs battery, based on the daily electricity price forecast. It can be noticed, that in days that the electricity price forecast has small or no fluctuation, the ESUs are not fully utilized. As well as, ESUs size differs for each day, because of the varying forecast of the electric vehicles' number, connected to the parking lot. Finally, the minimum state of charge of the equivalent ESUs battery of the microgrid ($\underline{SOC}_{ESS} + SOC_{l,EVPB}$) varies, in Figure 5.33, during the week because it's based on the microgrid's energy needs of each day.

In Table 5.3, the total microgrid operation costs can be observed of scenario I, scenario II and scenario III for a week.

Table 5.3 Total cost of microgrid's operation of the three different scenarios for a week

Microgrid operating cost during 4th -10th of July 2019 (€)	Scenario I	Scenario II	Scenario III
	2,347.4	2,355.7	3,584.4

6.
CONCLUSIONS

This thesis focuses on the development of a microgrid energy management system, that consists of large office buildings, photovoltaics, wind generators, building energy storage systems and electric vehicle parking lots. The proposed energy management system, targets to minimize the microgrid's total operating cost, with the use of the Particle Swarm Optimization (PSO) algorithm.

In order to optimize the microgrid's operation, it was needed to use forecasts of the energy generation of RES and the energy demands of the buildings. So, electricity price, ambient temperature, sun radiation and wind velocity forecasts of 15th of July 2019 have been used, to create the power generation and consumption profiles. Also, forecasts for the number of people working in the buildings and the electric vehicles connected to the parking lot have been created to calculate buildings' energy needs and microgrid's equivalent electric vehicle parking lot battery, respectively.

HVAC and non-Critical electrical load consumptions were optimized in the first level of optimization with the use of the PSO algorithm, by optimally distributing the power consumption throughout the day. The total electrical energy cost, deriving from HVAC system and non-Critical electrical loads, constituted the objective function that the PSO algorithm was called to minimize in the first level of optimization.

Energy flows from or to ESUs, were optimized in the second level of optimization again with the use of the PSO algorithm. More specifically, microgrid's energy cost consists of the buildings' energy demands cost, the profit of selling RESs' energy to the grid, the cost of charging the ESUs and the profit of selling ESUs' saved energy. Hence, the total microgrid energy cost constituted the objective function that PSO algorithm was called to minimize in the second level of optimization.

A set of constraints related with ESS, EVs' batteries, HVAC system and non-Critical electrical loads' time period shifting was applied to the optimization levels.

In order to evaluate the proposed energy management system, three scenarios were run at Matlab. These scenarios are examining the power management of the described microgrid assuming power supply interruptions, and the operation of a microgrid without any level of optimization for scenario I, scenario II and scenario III respectively. Assuming that scenario III is the typical operation of a microgrid today, in scenario I 187.39 €/day (40.16 %) can be saved. While, can be saved 176.83 €/day (37.47 %) in scenario II.

Another scenario was also run in Matlab, assuming the time period of 4^{th}-10^{th} of July 2019. This scenario simulates the operation of the microgrid for a week, using the three previous scenarios. The total microgrid week costs for the three scenarios, presented a cost decrease of 1,237.4 €/week (41.7 %) between scenario I and scenario III and a cost decrease of 1,228.7 €/week (41.36 %) between scenario II and scenario III.

In days with high electricity price fluctuations, the energy management system achieves a significant cost decrease because HVAC and non-Critical electrical loads can be shifted to time periods of low price and ESUs can be charged as long as electricity price is low and discharge (sell) while electricity price its high. It can also be seen that the microgrid doesn't make use of its whole capabilities in days that the electricity price has small or no fluctuations.

Also, the use of the optimization algorithm makes possible to use a smaller HVAC system in scenario I (40-45 kW in each thermal zone), compared to scenario III that a 100 kW system was needed to keep the internal temperature of each thermal zone into the permissible level as it had to withstand the thermal inertia of buildings in short time periods.

Finally, by having a power supply interruption, in scenario II, the energy management system charges appropriately the ESUs in order to cover the 75% of the buildings' energy needs during this period. This leads to a cost increase, in comparison to scenario I, because the system is forced to buy from the utility grid not optimally or during time periods that electricity price is high.

To extend the subject of this thesis in the future, a real-time HVAC system configuration could be introduced. Also, in order to make the prediction model of electrical needs more accurate, the stochastic behavior of people can be modeled. Finally, different types of buildings, apart from office buildings used in the present work, can be modeled and their respective energy needs be investigated.

7.

REFERENCES

[1] D. Thomas, O. Deblecker, C.S. Ioakimidis, "Optimal operation of an energy management system for a grid-connected smart building considering photovoltaics' uncertainty and stochastic electric vehicles' driving schedule," *Applied Energy*, vol. 210, pp. 1188-1206, Jan. 2018, DOI: 10.1016/j.apenergy.2017.07.035.

[2] Y. Xiang, J. Liu, Y. Liu, "Robust Energy Management of Microgrid with Uncertain Renewable Generation and Load," *IEEE Transactions on Smart Grid*, vol. 7, no. 2, pp. 1034-1043, March. 2016, DOI: 10.1109/TSG.2014.2385801.

[3] F. D. Kanellos, "Multiagent-System-Based Operation Scheduling of Large Ports' Power Systems with Emissions Limitation", *IEEE Systems Journal*, 13 (2), pp. 1831-1840, 2019.

[4] F. D. Kanellos, E. S. M. Volanis, and N. Hatziargyriou, "Power management method for large ports with multi-agent systems," *IEEE Trans. Smart Grid*, vol. 10, no 2, pp. 1259-1268, March, 2019

[5] S. G. Gennitsaris, F. D. Kanellos, "Emission-Aware and Cost-Effective Distributed Demand Response System for Extensively Electrified Large Ports", *IEEE Transactions on Power Systems*, 34 (6), pp. 4341-4351, 2019.

[6] F. Sehar, M. Pipattanasomporn, S. Rahman, "Coordinated control of building loads, PVs and ice storage to absorb PEV penetrations," *Int. Journal of Electrical Power and Energy Systems*, vol. 95, pp. 394-404, Feb. 2018, DOI: 10.1016/j.ijepes.2017.09.009.

[7] F. Farmani, M. Parvizimosaed, H. Monsef, A. Rahimi-Kian, "A conceptual model of a smart energy management system for a residential building equipped with CCHP system," *Int. Journal of Electrical Power and Energy Systems*, vol. 95, pp. 523-536, Feb. 2018, DOI: 10.1016/j.ijepes.2017.09.016.

[8] J. Romaní, M. Belusko, A. Alemu, L.F. Cabeza, A. de Gracia, F. Bruno, "Control concepts of a radiant wall working as thermal energy storage for peak load shifting of a heat pump coupled to a PV array," *Renewable Energy*, vol. 118, pp. 489-501, Apr. 2018, DOI: 10.1016/j.renene.2017.11.036.

[9] R. Tang, S. Wang, C. Yan, “A direct load control strategy of centralized air-conditioning systems for building fast demand response to urgent requests of smart grids,” *Automation in Construction*, vol. 87, pp. 74-83, March 2018, DOI: 10.1016/j.autcon.2017.12.012.

[10] C.D. Korkas, S. Baldi, I. Michailidis, E.B. Kosmatopoulos, “Occupancy-based demand response and thermal comfort optimization in microgrids with renewable energy sources and energy storage,” *Applied Energy*, vol. 163, pp. 93-104, Feb. 2016, DOI: 10.1016/j.apenergy.2015.10.140.

[11] C. Marino, M. Marufuzzaman, M. Hu, M.D. Sander, “Developing a CCHP-microgrid operation decision model under uncertainty,” *Computers and Industrial Engineering*, vol. 115, pp. 354-367, Jan. 2018, DOI: 10.1016/j.cie.2017.11.021.

[12] A. Mohsenzadeh, C. Pang, “Two stage residential energy management under distribution locational marginal pricing,” *Electric Power Systems Research*, vol. 154, pp. 361-372, Jan. 2018, DOI: 10.1016/j.epsr.2017.09.010.

[13] X. Jin, J. Wu, Y. Mu, M. Wang, X. Xu, H. Jia, “Hierarchical microgrid energy management in an office building,” *Applied Energy*, vol. 208, pp. 480-494, Dec. 2017, DOI: 10.1016/j.apenergy.2017.10.002.

[14] M. Martinez-Padon, T. Eveleigh, B. Tanju, “Optimizing residential energy management using an autonomous scheduler system,” *Expert Systems with Applications*, vol. 96, pp. 373-387, Apr. 2018, DOI: 10.1016/j.eswa.2017.12.017.

[15] L. Li, H. Mu, W. Gao, M. Li, “Optimization and analysis of CCHP system based on energy loads coupling of residential and office buildings,” *Applied Energy*, vol. 136, pp. 206-216, Dec. 2014, DOI: 10.1016/j.apenergy.2014.09.020.

[16] K.R. Khan, A. Rahman, A. Nadeem, M.S. Siddiqui, R.A. Khan (2018, August). Remote Monitoring and Control of Microgrid using Smart Sensor Network and Internet of Thing. Presented at 1st ICCAIS. [Online]. DOI: 10.1109/CAIS.2018.8441994.

[17] Q. Jiang, M. Xue, G. Geng, “Energy Management of Microgrid in Grid-Connected and Stand-Alone Modes,” *IEEE Transactions on Power Systems*, vol. 28, no. 3, pp. 3380–3389, 2013, DOI: 10.1109/tpwrs.2013.2244104.

[18] W. Shi, N. Li, C.-C. Chu, R. Gadh, “Real-Time Energy Management in Microgrids,” *IEEE Transactions on Smart Grid*, vol. 8, no. 1, pp. 228–238, Jan. 2017, DOI: 10.1109/tsg.2015.2462294.